

# Clusters beat Trend!?

## Testing feature hierarchy in statistical graphics

Susan VanderPlas\*

Department of Statistics and Statistical Laboratory, Iowa State University  
and

Heike Hofmann

Department of Statistics and Statistical Laboratory, Iowa State University

February 10, 2016

### Abstract

Graphics are very effective for communicating numerical information quickly and efficiently, but many of the design choices we make are based on subjective measures, such as personal taste or conventions of the discipline rather than objective criteria. We briefly introduce perceptual principles such as preattentive features and gestalt heuristics, and then discuss the design and results of a factorial experiment examining the effect of plot aesthetics such as color and trend lines on participants' assessment of ambiguous data displays. The quantitative and qualitative experimental results strongly suggest that plot aesthetics have a significant impact on the perception of important features in data displays.

*Keywords:* Visual inference, Lineup protocol, Preattentive Features, Saliency of Plot Aesthetics, User Study.

---

\*The authors gratefully acknowledge funding from the National Science Foundation Grant # DMS 1007697. All data collection has been conducted with approval from the Institutional Review Board IRB 10-347

# 1 Introduction and Background

Limits on attention span, short term memory, and information storage mechanisms within the human brain make it difficult for us to process numerical information in raw form effectively. (Well-designed) data displays are much better suited for this kind of communication, as they serve as a form of external cognition (Zhang, 1997; Scaife and Rogers, 1996), ordering and visually summarizing data and thereby invoking our higher-bandwidth visual system.

One fantastic example of this phenomenon is the Hertzsprung-Russell (HR) diagram, which was described as “one of the greatest observational syntheses in astronomy and astrophysics” because it allowed astronomers to clearly relate the absolute magnitude of a star to its’ spectral classification; facilitating greater understanding of stellar evolution (Spence and Garrison, 1993). The data it displayed was previously available in several different tables; but when plotted within the same chart, information that was invisible in a tabular representation became immediately clear (Lewandowsky and Spence, 1989b). Graphical displays more efficiently utilize cognitive resources by reducing the burden of storing, ordering, and summarizing raw data; this frees bandwidth for higher levels of information synthesis, allowing observers to note outliers, understand relationships between variables, and form new hypotheses.

Statistical graphics are powerful because they efficiently and effectively convey numerical information, but there exists relatively sparse empirical information about how the human perceptual system processes these displays. Our understanding of the perception of statistical graphics is informed by general psychological and psychophysics research as well as more specific research into the perception of data displays (Cleveland and McGill, 1984).

One relevant focus of psychological research is preattentive perception, that is, perception which occurs automatically in the first 200 ms of exposure to a visual stimulus (Treisman, 1985).

Research into **preattentive perception** provides us with some information about the temporal hierarchy of graphical feature processing. Color, line orientation, and shape are processed preattentively; that is, within 200 ms, it is possible to identify a single target

in a field of distractors, if the target differs with respect to color or shape (Goldstein, 2009). Research by Healey and Enns (1999) extends this work, demonstrating that certain features of three-dimensional data displays are also processed preattentively. However, neither target identification nor three-dimensional data processing always translate into faster or more accurate inference about the data displayed, particularly when participants have to integrate several preattentive features to understand the data.

**Feature detection** at the attentive stage of perception has also been examined in the context of statistical graphics; researchers have evaluated the perceptual implications of utilizing color, fill, shapes, and letters to denote categorical or stratified data in scatterplots. Cleveland and McGill (1984) ranked the optimality of these plot aesthetics based on response accuracy, preferring colors, amount of fill, shapes, and finally letters to indicate category membership. Lewandowsky and Spence (1989a) examined both accuracy and response time, finding that color is faster and more accurately perceived (except by individuals with color deficiency). Shape, fill, and discriminable letters (letters which do not share visual features, such as HQX) were identified as less accurate than color, while confusable letters (such as HEF) result in significantly decreased accuracy.

**Gestalt psychology** is another area of psychological research, that examines perception as a holistic experience, establishing and evaluating mental heuristics used to transform visual stimuli into useful, coherent information. Gestalt rules of perception can be easily applied to statistical graphics, as they describe the way we organize visual input, focusing on the holistic experience rather than the individual perceptual features.

For example, rather than perceiving four legs, a tail, two eyes, two ears, and a nose, we perceive a dog. This is due to certain perceptual heuristics, which provide a “top-down” method of understanding visual stimuli by taking into account past experience.

The rules of perceptual organization relevant to graphical perception in this experiment are:

- **Proximity:** two elements which are close together are more likely to belong to a single unit.
- **Similarity:** the more of the same or similar aesthetics two elements share two elements are, the more likely they belong to a single unit.

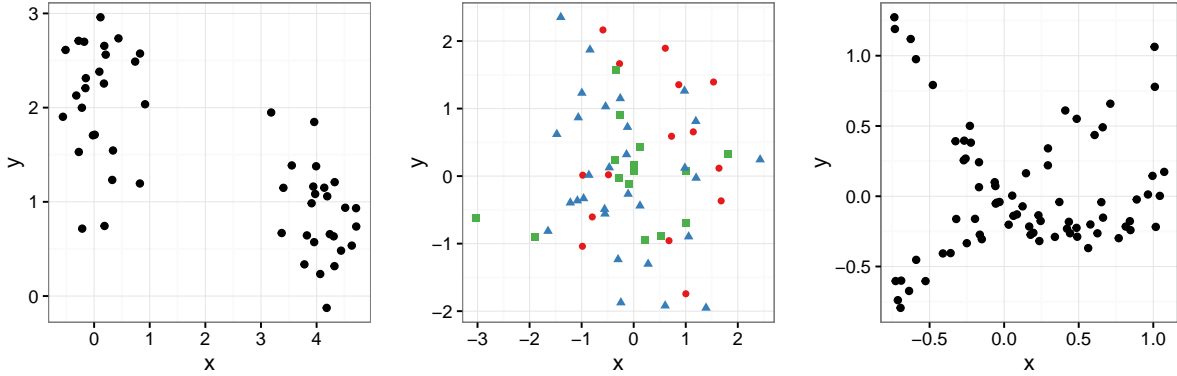


Figure 1: *Proximity* renders the fifty points of the first scatterplot as two distinct (and equal-sized) groups. Shapes and colors create three groups of points in the middle scatterplot by invoking the Gestalt principle of *Similarity*. *Good Continuation* renders the points in the scatterplot on the right hand side into two groups of points on curves: one a straight line with an upward slope, the other a curve that initially decreases and at the end of the range shows an uptick.

- **Good continuation:** two elements which blend together smoothly likely belong to one unit.
- **Common region:** elements contained within a common region likely belong together.

A complete list of the rules of perceptual grouping can be found in Goldstein (2009).

The plots in Figure 1 demonstrate several of the gestalt principles which combine to order our perceptual experience from the top down. These laws help to order our perception of charts as well: points which are colored or shaped the same are perceived as belonging to a group (similarity), points within a bounding interval or ellipse are perceived as belonging to the same group (common region), and regression lines with confidence intervals are perceived as single units (continuity and common region).

The processing of visual stimuli utilizes low-level feature detection, which occurs automatically in the preattentive perceptual phase, and higher-level mental heuristics which are informed by experience. Both types of mental processes utilize physical location, color, and shape to organize perceptual stimuli and direct attention to graphical features which stand out.

Research on preattentive perception is important because features that are perceived

preattentively require less mental effort to process from raw visual stimuli than non-preattentive features. Top-down gestalt heuristics are subsequently applied to the categorized features in order to make sense of the visual scene once the attentive stage of perception is reached.

There are two sequential transitions here that should either be combined or separated a bit... I'm still considering how to do this well.

This paper describes the design and the results of a user study exploring the hierarchy of gestalt principles in the perception of statistical graphics. We utilize information from previous studies (Demiralp et al., 2014; Robinson, 2003; Healey et al., 1996) concerning the hierarchy of preattentive feature perception in order to maximize the effect of preattentive feature differences.

Statistical graphics can be difficult to examine experimentally; qualitative studies rely on descriptions of the plot by participants who may not be able to articulate their observations precisely, while quantitative studies may only be able to examine whether the viewer can accurately read numerical information from the chart, instead of exploring the overall utility of the data display holistically. Here, we are describing the setup and results of a study using statistical lineup methodology to provide quantitative and qualitative information.

**Statistical lineups** are an important experimental tool for quantifying the significance of a finding in a graphical display. Lineups fuse commonly used psychological tests (target identification, visual search) (Vanderplas and Hofmann, 2016) with statistical hypothesis tests, thereby enabling formal experimental evaluation of statistical graphics.

Lineups are an experimental tool designed to serve as a visually conducted hypothesis test, separating significant effects from those that would be expected under a null hypothesis (Buja et al., 2009; Majumder et al., 2013; Hofmann et al., 2012; Wickham et al., 2010). A statistical lineup consists of (usually) 20 sub-plots, arranged in a grid (examples are shown in Figure 6). Of these plots, one plot is the “target plot”, generated from either real data or an alternate model (equivalent to  $H_A$  in hypothesis testing); the other 19 plots are generated either using bootstrap samples of the real data or by generating “true null” plots from the null distribution  $H_0$ . If a participant can identify the target plot from

the field of distractors, this counts as evidence against the null hypothesis. Based on the number of evaluations and the number of target identifications, significance of a finding is then determined in the same sense as for a conventional hypothesis test. Performance on lineups has been shown to depend primarily on logical reasoning ability, and does not depend significantly on statistical training (Vanderplas and Hofmann, 2016).

Apart from the hypothesis testing construct, the use of statistical lineups to test statistical graphics conforms nicely to psychological testing constructs such as visual search (DeMita et al., 1981; Treisman and Gelade, 1980), where a single target is embedded in a field of distractors and response time, accuracy, or both are used to measure the complexity of the underlying psychological processes leading to identification.

In this paper we **modify the lineup protocol** by introducing a second target to each lineup. The two targets represent two different, competing signals; an observer’s choice then demonstrates empirically which signal is more salient. Cognitively, the presence of two targets leads to a dual-target search scenario (Fleck et al., 2010), which effectively introduces a ‘masking’ effect where the more salient target is selected and the search for more targets stops (“satisfaction of search”), i.e. people tend to pick the more salient target and not notice the second target, even though in the absence of the more salient target they would have picked it out.

From a statistical perspective, this is analogous to a Bayesian framework in which the relative strengths of two competing models are evaluated by a comparison with each other and with a common null.

In the present study, participants were allowed to submit multiple selections to prevent any forced-choice scenario which might skew the results. However, only 0.6% of the evaluations resulted in an identification of both targets.

The search for multiple targets is a more demanding cognitive task (Cain et al., 2011) that is more sensitive to contextual effects (Adamo et al., 2015), but without any time constraints imposed by the experimental protocol, participants can be expected to identify at least one of the plots with accuracy comparable to a single-target search task.

Using this testing framework, we apply different aesthetics, such as color and shape, as well as plot objects which display statistical calculations, such as trend lines and bounding

ellipses. These additional plot layers, discussed in more detail in the next section, are designed to emphasize one of the two competing targets and affect the overall visual signal of the target plot relative to the null plots. We expect that in a situation similar to the third plot of Figure 1, the addition of two trend lines would emphasize the “good continuation” of points in the plot, producing a stronger visual signal, even though the underlying data has not changed. Similarly, the grouping effect in the first plot in the figure should be enhanced if the points in each group are colored differently, as this adds similarity to the proximity heuristic. In plots that are ambiguous, containing some clustering of points as well as a linear relationship between  $x$  and  $y$ , additional aesthetic cues may “tip the balance” in favor of recognizing one type of signal over the other.

The study in this paper is designed to inform our understanding of the perceptual implications of these additional aesthetics, in order to provide guidelines for the creation of data displays which provide visual cues consistent with gestalt heuristics and preattentive perceptual preferences.

The next section discusses the particulars of the experimental design, including the data generation model, plot aesthetics, selection of color and shape palettes, and other important considerations. Experimental results are presented in section 3, and implications and conclusions are discussed in section 4.

## 2 Experimental Setup and Design

In this section, we discuss the models generating data for the two types of signal plots and the null plots, the selection of plot aesthetic combinations and aesthetic values, and the design and execution of the experiment.

### 2.1 Data Generation

Conventional lineups require a single “target” data set and a method for generating null plots. When utilizing real data for target plots, null plots are often generated through permutations.

Here, it is possible to generate true null plots from a null model that do not depend on

the data used in the target plot. This experiment measures two competing gestalt heuristics, proximity and good continuation, using two data-generating models. Both models provide data in the same range of values in  $X$  and  $Y$ ;  $M_C$  generates data with  $K$  clusters, while  $M_T$  generates data with a positive linear relationship between  $X$  and  $Y$ . Null datasets are created using a mixture model  $M_0$  which combines  $M_C$  and  $M_T$ . In order to facilitate mixing these two models, controls on cluster centers generated by  $M_C$  ensure that  $X$  and  $Y$  have a positive linear relationship with a correlation  $\rho \in (0.25, 0.75)$ , similar to the linear relationship between datasets generated by  $M_0$ .

These constraints provide some assurance that participants who select a plot with data generated from  $M_T$  are doing so because of visual cues indicating a linear trend (rather than a lack of clustering compared to plots with data generated from  $M_0$ ), and participants who select a plot with data generated from  $M_C$  are doing so because of visual cues indicating clustering, rather than a lack of a linear relationship relative to plots with data generated from  $M_0$ .

### 2.1.1 Regression Model $M_T$

This model has the parameter  $\sigma_T$  to reflect the amount of scatter around the trend line. It generates  $N$  points  $(x_i, y_i), i = 1, \dots, N$  where  $x$  and  $y$  have a positive linear relationship. The data generation mechanism is as follows:

#### Algorithm 2.1

*Input Parameters:* sample size  $N$ ,  $\sigma_T$  standard deviation around the linear trend

*Output:*  $N$  points, in form of vectors  $x$  and  $y$ .

1. Generate  $\tilde{x}_i, i = 1, \dots, N$ , as a sequence of evenly spaced points in  $[-1, 1]$ .  
*This step ensures that the full range in  $x$  is used, which in turn keeps the ratio of  $x$  to  $y$  range constant.*
2. Jitter  $\tilde{x}_i$  by adding small uniformly distributed perturbations to each of the values:  
 $x_i = \tilde{x}_i + \eta_i$ , where  $\eta_i \sim \text{Unif}(-z, z)$ ,  $z = \frac{2}{5(N-1)}$ .
3. Generate  $y_i$  as a linear regressand of  $x_i$ :  $y_i = x_i + e_i$ ,  $e_i \sim N(0, \sigma_T^2)$ . Several values of  $\sigma_T^2$  are shown in Figure 2.



#### 4. Center and scale $x_i, y_i$ .

We compute the coefficient of determination for all of the plots to assess the amount of linearity in each panel, computed as

$$R^2 = 1 - \frac{RSS}{TSS}, \quad (1)$$

where TSS is the total sum of squares,  $TSS = \sum_{i=1}^N (y_i - \bar{y})^2$  and  $RSS = \sum_{i=1}^N e_i^2$ , the residual sum of squares. The expected value of the coefficient of determination  $E[R^2]$  in this scenario is

$$E[R^2] = \frac{1}{1 + 3\sigma_T^2},$$

because  $E[RSS] = N\sigma_T^2$  and  $E[TSS] = \sum_{i=1}^N E[y_i^2]$  (as  $E[Y] = 0$ ), where

$$E[y_i^2] = E[x_i^2 + e_i^2 + 2x_i e_i] = \frac{1}{3} + \sigma_T^2.$$

The use of  $R^2$  to assess the strength of the linear relationship (rather than the correlation) is indicated because human perception of correlation strength more closely aligns with  $R^2$  (Bobko and Karren, 1979; Lewandowsky and Spence, 1989b).

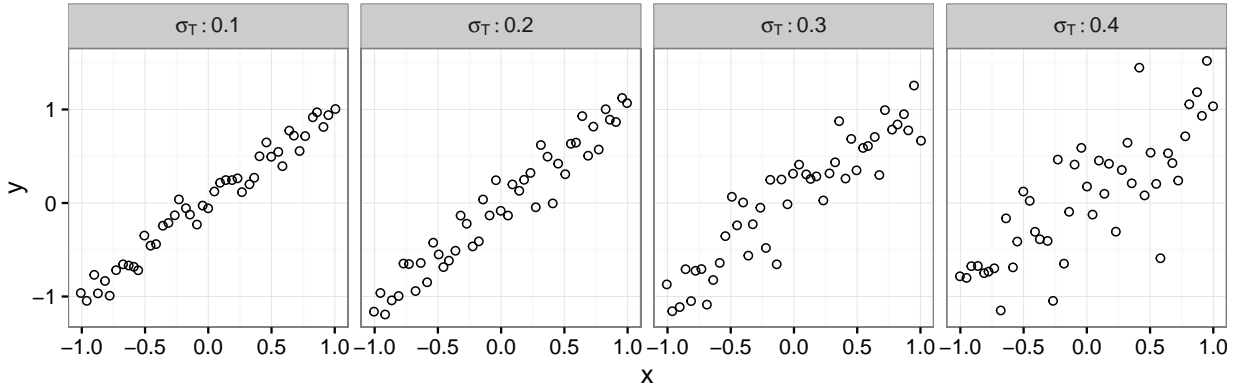


Figure 2: Set of scatterplots showing one draw each from the trend model  $M_T$  for parameter values of  $\sigma_T \in \{0.1, 0.2, 0.3, 0.4\}$ .

#### 2.1.2 Cluster Model $M_C$

We begin by generating  $K$  cluster centers on a  $K \times K$  grid, then we generate points around selected cluster centers.

## Algorithm 2.2

*Input Parameters:*  $N$  points,  $K$  clusters,  $\sigma_C$  cluster standard deviation

*Output:*  $N$  points, in form of vectors  $x$  and  $y$ .

1. Generate cluster centers  $(c_i^x, c_i^y)$  for each of the  $K$  clusters,  $i = 1, \dots, K$ :
  - (a) in form of two vectors  $c^x$  and  $c^y$  of permutations of  $\{1, \dots, K\}$ , such that
  - (b) the correlation between cluster centers  $\text{cor}(c^x, c^y)$  falls into a range of  $[-.25, .75]$ .
2. Center and standardize cluster centers  $(c^x, c^y)$ :

$$\tilde{c}_i^x = \frac{c_i^x - \bar{c}}{s_c} \quad \text{and} \quad \tilde{c}_i^y = \frac{c_i^y - \bar{c}}{s_c},$$

where  $\bar{c} = (K + 1)/2$  and  $s_c^2 = \frac{K(K+1)}{12}$  for all  $i = 1, \dots, K$ .

3. For the  $K$  clusters, we want to have nearly equal sized groups, but allow some variability. Cluster sizes  $g = (g_1, \dots, g_K)$  with  $N = \sum_{i=1}^K g_i$ , for clusters  $1, \dots, K$  are therefore determined as a draw from a multinomial distribution:

$$g \sim \text{Multinomial}(K, p) \text{ where } p = \tilde{p} / \sum_{i=1}^K \tilde{p}_i, \text{ for } \tilde{p} \sim N\left(\frac{1}{K}, \frac{1}{2K^2}\right).$$

4. Generate points around cluster centers by adding small normal perturbations:

$$\begin{aligned} x_i &= \tilde{c}_{g_i}^x + e_i^x, \text{ where } e_i^x \sim N(0, \sigma_C^2), \\ y_i &= \tilde{c}_{g_i}^y + e_i^y, \text{ where } e_i^y \sim N(0, \sigma_C^2). \end{aligned}$$

5. Center and scale  $x_i, y_i$ .

As a measure of cluster cohesion we use a coefficient to assess the amount of variability within each cluster, compared to total variability. Note that for the purpose of clustering, variability is measured as the variability in both  $x$  and  $y$  from a common mean, i.e. we implicitly assume that the values in  $x$  and  $y$  are on the same scale. This ensures that  $\sigma_C$  is a scaling parameter that regulates the amount of cluster cohesion (see Figure 3).

For two numeric variables  $x$  and  $y$  and grouping variable  $g$  with  $g_i \in \{1, \dots, K\}, i = 1, \dots, n$ , we compute the *cluster index*  $C^2$  as follows: let  $j(i)$  be the function that maps

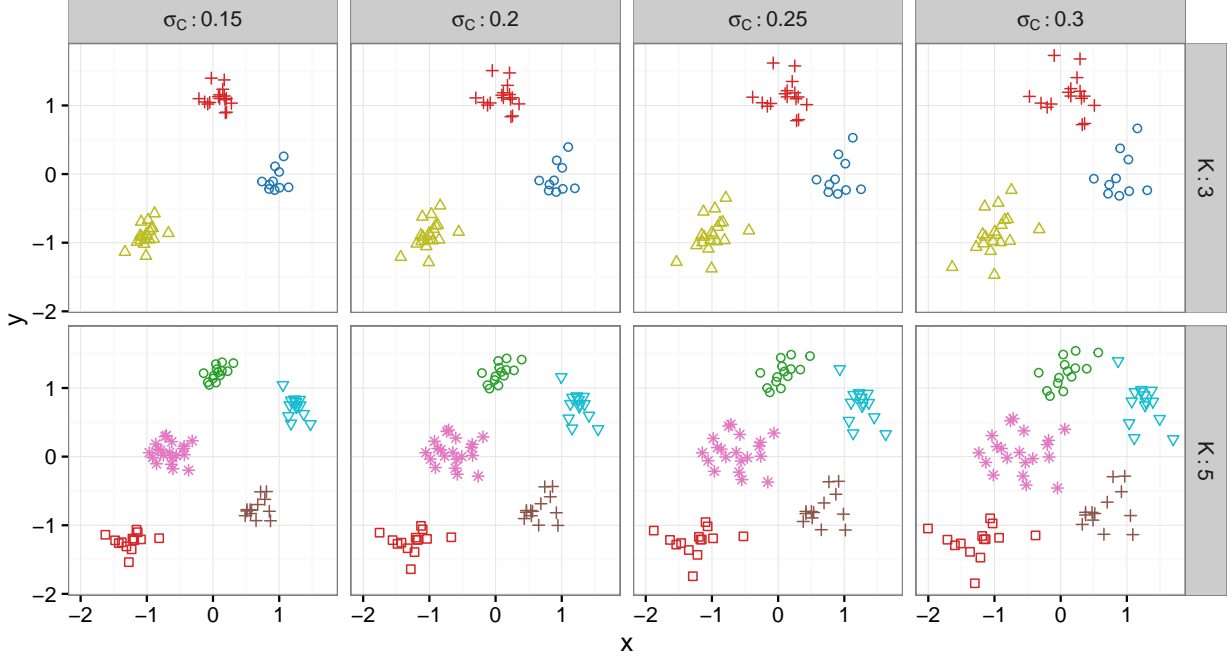


Figure 3: Scatterplots of clustering output for different inner cluster spread  $\sigma_C$  (left to right) and different number of clusters  $K$  (top and bottom), generated using the same random seed at each parameter setting. The colors and shapes shown are those used in the lineups for  $K = 3$  and  $K = 5$ .

index  $i = 1, \dots, n$  to one of the clusters  $1, \dots, K$  given by the grouping variable  $g$ . Then for each level of  $g$ , we find a cluster center as  $\bar{x}_{j(i)}$  and  $\bar{y}_{j(i)}$ , and we determine the strength of the clustering by comparing the within cluster variability with the overall variability:

$$\begin{aligned}
 C^2 &= 1 - \frac{CSS}{TSS}, \\
 CSS &= \sum_{i=1}^n \left( x_{j(i)} - \bar{x}_{j(i)} \right)^2 + \left( y_{j(i)} - \bar{y}_{j(i)} \right)^2, \\
 TSS &= \sum_{i=1}^n \left( x_i - \bar{x} \right)^2 + \left( y_i - \bar{y} \right)^2.
 \end{aligned} \tag{2}$$

The cluster index  $C^2$ , which is approximately inversely linear in  $\sigma_C^2$ , measures the actual amount of clustering in the generated data.

### 2.1.3 Null Model $M_0$

The generative model for null data is a mixture model  $M_0$  that draws  $n_c \sim \text{Binomial}(N, \lambda)$  observations from the cluster model, and  $n_T = N - n_c$  from the regression model  $M_T$ . Observations are assigned to specific clusters using hierarchical clustering, which creates groups consistent with any structure present in the generated data. This provides a plausible grouping for use in aesthetic and statistics requiring categorical data (color, shape, bounding ellipses).

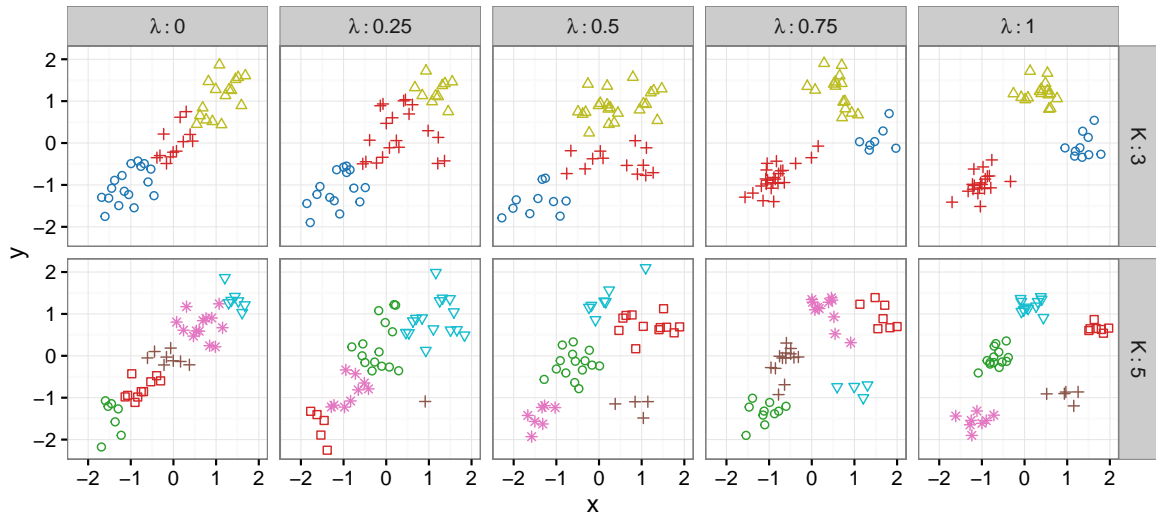


Figure 4: Scatterplots of data generated from  $M_0$  using different values of  $\lambda$ , generated using the same random seed at each  $\lambda$  value.

Null data in this experiment is generated using  $\lambda = 0.5$ , that is, each point in a null data set is equally likely to have been generated from  $M_C$  and  $M_T$  to ensure maximal distance of the null plots from either target.

### 2.1.4 Parameters used in Data Generation

Models  $M_C$ ,  $M_T$ , and  $M_0$  provide the foundation for this experiment; by manipulating cluster standard deviation  $\sigma_C$  and regression standard deviation  $\sigma_T$  for varying numbers of clusters  $K = 3, 5$ , we systematically control the statistical signal present in the target plots and generate corresponding null plots that are mixtures of the two distributions. For each parameter set  $\{K, N, \sigma_C, \sigma_T\}$ , as described in Table 1, we generate a lineup dataset consisting of one set drawn from  $M_C$ , one set drawn from  $M_T$ , and 18 sets drawn from  $M_0$ .

Parameter	Description	Choices
$K$	# Clusters	3, 5
$N$	# Points	$15 \cdot K$
$\sigma_T$	Scatter around trend line	.25, .35, .45
$\sigma_C$	Scatter around cluster centers	.25, .30, .35 ( $K = 3$ ) .20, .25, .30 ( $K = 5$ )

Table 1: Parameter settings for generation of lineup datasets.

The parameter values were chosen in an approach similar to that taken in Roy Chowdhury et al. (2014): for each combination of  $\sigma_T \in \{0.2, 0.25, \dots, 0.5\}$ ,  $\sigma_C \in \{0.1, 0.15, \dots, 0.4\}$ , and  $K \in \{3, 5\}$  we simulated 1000 lineup datasets. Then trend and cluster strength indices,  $R^2$  and  $C^2$ , were computed for the simulated target plots, and compared to the most extreme value for each of the 18 null plots of the same lineup data.

The resulting distributions allow us to objectively assess the difficulty of detecting the target datasets computationally (without relying on human perception) within the full parameter space. That is, a target plot with  $R^2 = 0.95$  is very easy to identify when surrounded by null plots with  $R^2 = 0.5$ , while null plots with  $R^2 = 0.9$  make the target plot more difficult to identify.

Figure 5 shows densities of each measure computed from the maximum of 18 null plots compared to the measure in the signal plot for one combination of parameters. There is some overlap in the distribution of  $R^2$  for the null plots compared to the target plot displaying data drawn from  $M_T$ . As a result, the distribution of the cluster statistic values are more easily separated from the null data sets than the distribution of the trend statistic, e.g.  $\sigma_C = 0.20$  is producing cluster target data sets that are a bit easier to identify numerically than trend targets with a parameter value of  $\sigma_T = 0.25$ .

Graphical summaries of simulation results for a range of values for  $\sigma_C$  and  $\sigma_T$  are provided in Appendix A. Using information from the simulation, we identified values and generate lineup data sets for each  $\sigma_T$  and  $\sigma_C$  (as shown in Table 1) corresponding to “easy”, “medium” and “hard” numerical comparisons between corresponding target data sets and null data sets. It is important to note that the numerical measures we have described in

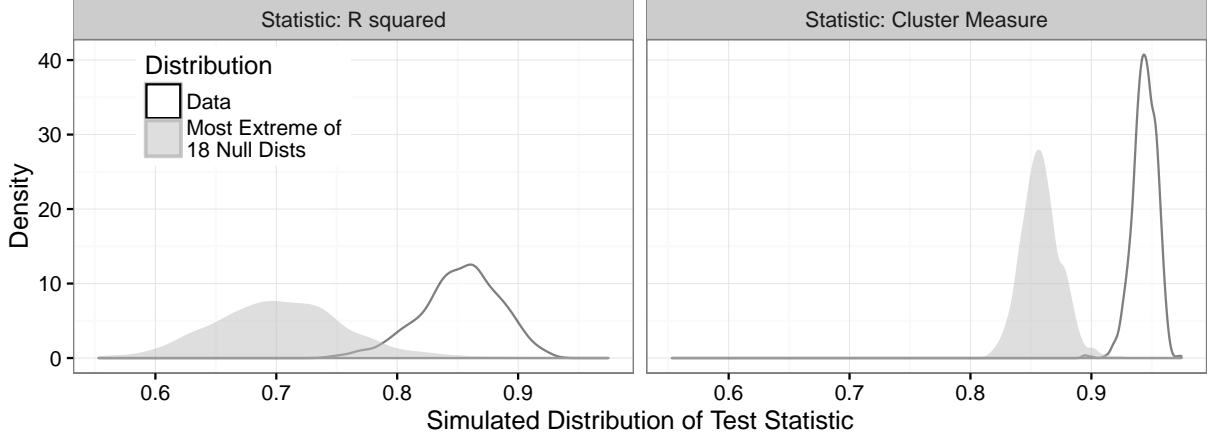


Figure 5: Density of test statistics measuring trend strength and cluster strength for target distributions and null plots based on 1,000 draws of lineup data with  $\sigma_T = 0.25$ ,  $\sigma_C = 0.20$  and  $K = 3$ .

equations (1) and (2) only provide information on the numerical discriminability of the target datasets from the null datasets; the simulation cannot provide us with exact information on the perceptual discriminability. It has been established that human perception of scatterplots does not replicate statistical measures exactly (Bobko and Karren, 1979; Mosteller et al., 1981; Lewandowsky and Spence, 1989b).

Each of the generated datasets is then plotted as a lineup using aesthetics which emphasize clusters and/or linear relationships, in order to experimentally determine how these aesthetics change a participant’s preference and ability to identify each target plot. The next section describes the aesthetic combinations and their anticipated effect on participant responses.

## 2.2 Lineup Rendering

### 2.2.1 Plot Aesthetics

Gestalt perceptual theory suggests that perceptual features such as shape, color, trend lines, and boundary regions modify the perception of ambiguous graphs, emphasizing clustering in the data (in the case of shape, color, and bounding ellipses) or linear relationships (in the case of trend lines and prediction intervals), as demonstrated in Figure 1. For each dataset we examine the effect of the plot aesthetics (color, shape) and statistical layers (trend line,

		Trend Emphasis		
		0	1	2
Cluster Emphasis	Strength			
	0	None	Trend	Trend + Error
	1	Color Shape	Color + Trend	
	2	Color + Shape Color + Ellipse		Color + Ellipse + Trend + Error
	3	Color + Shape + Ellipse		

Table 2: Plot aesthetics and statistical layers which impact perception of statistical plots, according to gestalt theory.

boundary ellipses, prediction intervals) shown in Table 2 on target identification. Examples of these plot aesthetics are shown in Figure 6.

We expect that relative to a plot with no extra aesthetics or statistical layers, the addition of color, shape, and 95% boundary ellipses increases the probability of a participant selecting the target plot with data generated from  $M_C$ , the cluster model, and that the addition of these aesthetics decreases the probability of a participant selecting the target plot with data generated from  $M_T$ , the trend model.

Similarly, we expect that relative to a plot with no extra aesthetics or statistical layers, the addition of a trend line and prediction interval (“error band”) increases the probability of a participant selecting the target plot with data generated from  $M_T$ , the trend model, and decreases the probability of a participant selecting the target plot with data generated from  $M_C$ , the cluster model.

### 2.2.2 Color and Shape Palettes

Colors and shapes used in this study were selected in order to maximize preattentive feature differentiation. Demiralp et al. (2014) provide sets of 10 colors and 10 shapes, with corresponding distance matrices, determined by user studies. Using these perceptual kernels for shape and color, we identified a maximally differentiable set of 3 and 5 colors each.

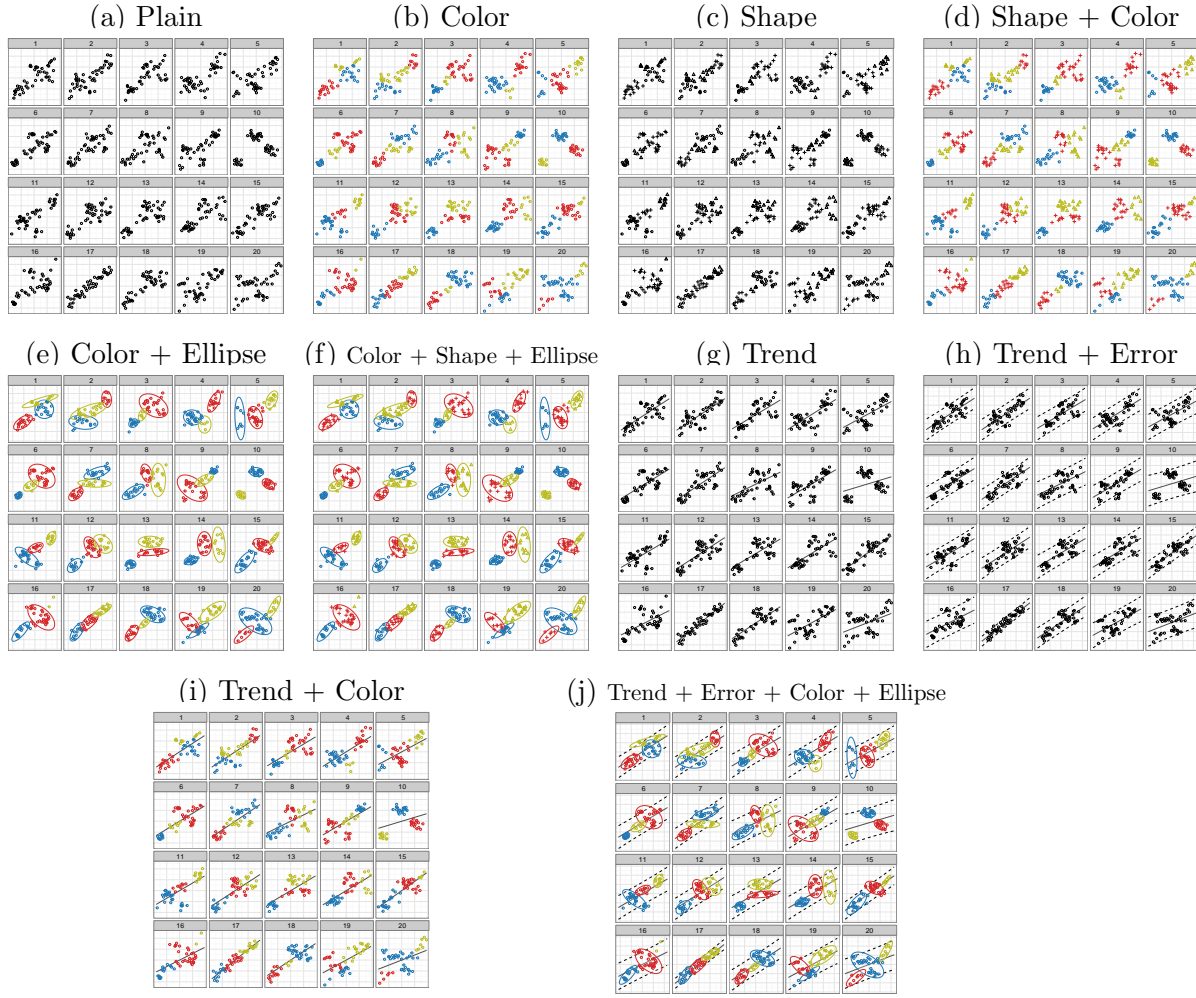
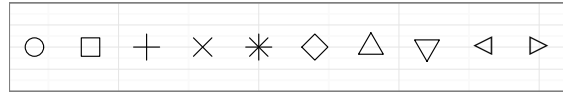


Figure 6: Overview of each of the 10 plot feature combinations compared in this study, with  $K = 3$ ,  $\sigma_T = 0.25$  and  $\sigma_C = 0.20$ .

Figure 7: Color and shape palettes investigated for differentiability in Demiralp et al. (2014).



(a) Color Palette. For the present study gray was removed from the palette to make the experiment more inclusive of participants with color deficiency.



(b) Shape palette. Due to varying point size between Unicode and non-Unicode characters, the last two shapes were not used in this study.



The color palette used in Demiralp et al. (2014) and shown in Figure 7a is derived from colors available in the visualization software Tableau (Hanrahan, 2003).

In order to produce experimental stimuli accessible to the approximately 4% of the population with red-green color deficiency (Gegenfurtner and Sharpe, 2001), we removed the gray hue from the palette, as gray is often difficult to distinguish from red and green for those with protanopia and deuteranopia, the most common types of colorblindness. This modification also resulted in maximally different color combinations that did not include red-green combinations, which would also impact the ability of color-deficient individuals to participate fully in this experiment.

Software compatibility issues led us to exclude two shapes used in Demiralp et al. (2014) and shown in Figure 7b. The left and right triangle shapes (available only in unicode within R) were excluded from our investigation due to size differences between unicode and non-unicode shapes. After optimization over the sum of all pairwise distances, the maximally different shape sequences for the 3 and 5 cluster datasets also conform to the guidelines in Robinson (2003): for  $K = 3$  the shapes are from Robinson’s group 1, 2, and 9, for  $K = 5$  the shapes are from groups 1, 2, 3, 9, and 10. Robinson’s groups are designed so that shapes in different groups show differences in preattentive properties; that is, they are easily distinguishable. In addition, all shapes are non-filled, making them consistent with one of the simplest solutions to overplotting of points in the tradition of Tukey (1977); Cleveland (1994) and Few (2009). For this reason we abstained from the additional use of alpha-blending of points to diminish the effect of overplotting in the plots.

## 2.3 Experimental Design

The study is designed hierarchically, as a factorial experiment for combinations of  $\sigma_C$ ,  $\sigma_T$ , and  $K$ , with three replicates at each parameter combination. These parameters are used to generate lineup datasets which serve as blocks for the plot aesthetic level of the experiment; each dataset is rendered with every combination of aesthetics described in Table 2. Participants are assigned to generated plots according to an augmented balanced incomplete block scheme: each participant is asked to evaluate 10 plots, which consist of one plot at each combination of  $\sigma_C$  and  $\sigma_T$ , randomized across levels of  $K$ , with one

additional plot providing replication of one level of  $\sigma_C \times \sigma_T$ . Each of a participant’s 10 plots presents a different aesthetic combination.

## 2.4 Hypotheses

The primary purpose of this study is to understand how visual aesthetics affect signal detection in the presence of competing signals. We expect that plot modifications which emphasize similarity and proximity, such as color, shape, and 95% bounding ellipses, increase the probability of detecting the clustering relationship, while plot modifications which emphasize good continuation, such as trend lines and prediction intervals, increase the probability of detecting the linear relationship.

A secondary purpose of the study is to relate signal strength (as determined by dataset parameters  $\sigma_C$ ,  $\sigma_T$ , and  $K$ ) to signal detection in a visualization by a human observer.

## 2.5 Participant Recruitment

Participants were recruited using Amazon’s Mechanical Turk service (Amazon, 2010), which connects interested workers with “Human Intelligence Tasks” (HITs), which are (typically) short tasks that are not easily automated. Only workers with at least 100 previous HITs at a 95% successful completion rate were allowed to sign up for completing the task. These restrictions reduce the amount of data cleaning required by ensuring that participants have experience with the Mechanical Turk system, as well as a vested interest in doing well.

Participants had to complete a pre-trial before being able to access the experiment. The lineups used in the pre-trial contained only a single target, and participants had to correctly identify the target in at least two lineups. The webpage used to collect data from Amazon Turk participants is available at <https://erichare.shinyapps.io/lineups/>. No data was recorded from the pre-trial because participants had not provided informed consent at this point.

Once participants completed the example task and provided informed consent, they could accept the HIT through Amazon and were directed to the main experimental task.

## 2.6 Task Description

Participants were required to complete ten lineups, answering “Which plot is the most different from the others?”. Participants were asked to provide a short reason for their choice, such as “Strong linear trend” or “Groups of points”, and to rate their confidence in their selection from 0 (least confident) to 5 (most confident). After the first question, basic demographic information was collected: age range, gender, and highest level of education.

Throughout the experiment, participants were not informed about the inclusion of a second target into the lineup plots. The small number of participants choosing multiple plots in their answer suggests that most participants did not discover that two target plots were present in each lineup and were thus naive to the true purpose of the experiment.

## 3 Results

### 3.1 General results & Demographics

Data collection was conducted over a 24 hour period, during which time 1356 individuals completed 13519 unique lineup evaluations. Participants who completed fewer than 10 lineups were removed from the study (159 participants, 1060 evaluations), and lineup evaluations in excess of 10 for each participant were also removed from the study (421 evaluations). After these data filtration steps, our data consist of 12010 trials completed by 1201 participants.

Of the participants who completed at least 10 lineup evaluations, 61% were male, relatively younger than the US population and relatively well educated (see Figure 8). Each plot was evaluated by between 11 and 36 individuals (Mean: 22.24, SD: 4.64). 82.9% of the participant evaluations identified at least one of the two target plots successfully (Trend: 26.8%, Cluster: 56.8%).

From Figure 9 we see that participants identified more cluster targets than trend targets (there were more aesthetics expected to emphasize clustering in the data), but also did not primarily identify one target type over the other. Generally a participant picked both types over the course of ten lineups.

For each design (aesthetic combination), we first consider the probability that a partic-

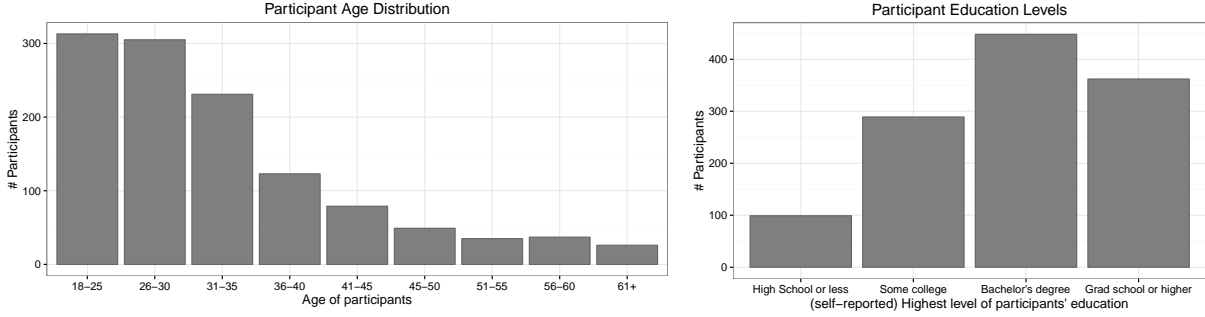


Figure 8: Basic demographics of participants.

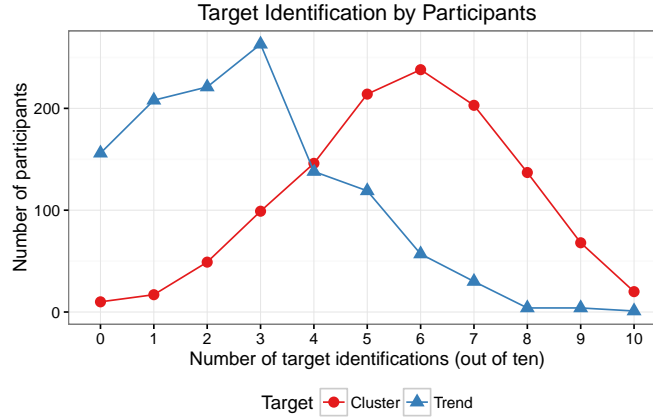


Figure 9: Target identifications by participants. Generally, participants are not primed for one target over the other.

ipant selects one of the two target plots, and then we consider the conditional probability of selecting the cluster target over the trend target.

### 3.2 Target Plot Identifications

In order to assess which of the two stimuli dominated in each of the designs, we concentrate first on all those responses in which participants identified at least one of the targets (9959 trials). Figure 10 shows an overview of the number of evaluations by design (outlines) and the number of times participants chose at least one of the targets (dark shaded areas). Designs associated with clustering as shown in Table 2 lead to significantly fewer correct evaluations ( $\chi^2_9 = 389$ ,  $p$ -value  $< 0.0001$ ). A possible cause for this is discussed in more detail in section 3.4.

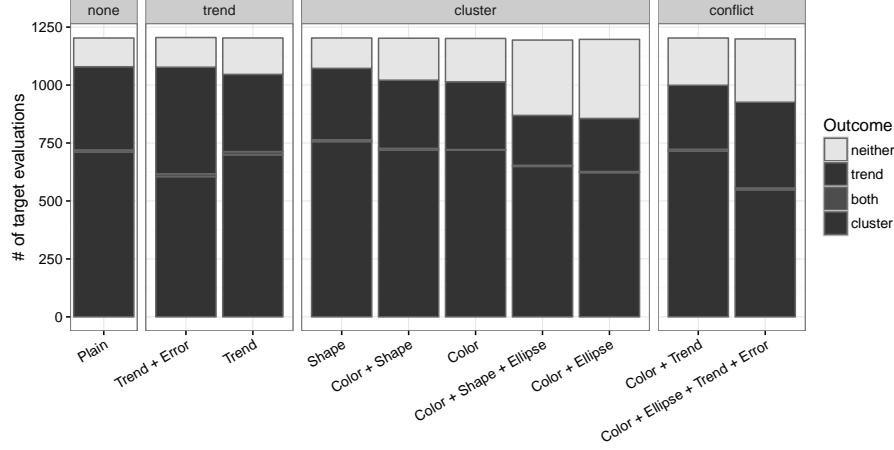


Figure 10: In dark: number of evaluations by design, in which at least one of the targets was identified. Each of the dark areas is split into two, according to the type of target, with evaluations where both targets were identified between the two. Due to the design of the experiment, each design was evaluated almost the same number of times (between 1195 and 1208 times, outlined rectangles).

### 3.3 Face-Off: Trend versus Cluster

For all trials in which at least one of the targets was correctly identified, we compare the probability of selecting the cluster target generated by  $M_C$  with the probability of selecting the trend target generated by  $M_T$ . Define  $C_{ijk}$  to be the event

$$\{\text{Participant } k \text{ selects the cluster target for dataset } j \text{ with aesthetic set } i\}$$

and  $T_{ijk}$  to be the analogous selection of the trend target. We model the cluster versus trend decision using a logistic regression with a random effect for each dataset to account for different difficulty levels in the generated data, and a random effect for participant to account for skill level, as shown in equation 3.

$$\text{logit } P(C_{ijk}|C_{ijk} \cup T_{ijk}) = \mathbf{W}\alpha + \mathbf{X}\beta + \mathbf{J}\gamma + \mathbf{K}\eta, \quad (3)$$

where

$\alpha$  is a vector of fixed effects  $(\mu, \alpha_T, \alpha_C, \alpha_K)$ .  $\mu$  is a baseline average of the probability to pick the cluster target over the trend target.  $\alpha_T$  and  $\alpha_C$  are parameters for the

effect of the standard error around trend lines  $s_T \in \{0.25, 0.35, 0.45\}$  and with cluster variability  $s_C \in \{0.2, 0.25, 0.3, 0.35\}$ , and  $\alpha_K$  is the effect of the number of clusters  $K \in \{3, 5\}$ .

$\beta_i$  describe plot aesthetics,

$\gamma_j \stackrel{iid}{\sim} N(0, \sigma_{\text{data}}^2)$ , random effect for dataset specific characteristics,

$\eta_k \stackrel{iid}{\sim} N(0, \sigma_{\text{participant}}^2)$ , random effect for participant characteristics,

$\epsilon_{ijk} \stackrel{iid}{\sim} N(0, \sigma_e^2)$ , error associated with a single trial evaluation.

We also assume that random effects for dataset and participant are orthogonal.

The estimated log odds of a decision in favor of cluster over trend target for each of the designs are shown in Figure 11. From left to right the (log) odds of selecting the cluster target over the trend target increase. As hypothesized, the strongest signal for identifying groups, is color + shape + ellipse, while trend + error results in the strongest signal in favor of trends. Most of the effects are not significantly different, as seen in the letter values (Piepho, 2004) based on Tukey’s Post Hoc difference tests on the left hand side of the figure, representing pairwise comparisons of all of the designs, adjusted for multiple comparison. The estimates for parameters  $\alpha_C$  and  $\alpha_T$ , quantifying the effect of increased variability within clusters and around the trend line, are highly significant and work as hypothesized: with an increase in the variability, the strength of the target’s signal decreases and correspondingly the probability for detecting the corresponding target decreases significantly (see Table 7 in appendix section C.4 for exact numbers and a discussion of further co-variates).

We found the interaction effects between a design and each of the parameters controlling variability,  $s_C$  and  $s_T$ , to be not significant, i.e. the results for the designs are stable in that sense, that it does not seem to matter how difficult (at least within our parameter setting) a lineup is. XXX Susan, do we want to include this? it’s in models gvl.4d and gvl.4e - I didn’t include those models in the paper yet, but they are in expanded-model.R. Numbers:  $s_T$ : plottype interaction: 11.15,9,0.2656  $s_C$ :plottype interaction: 6.9026,9,0.6473

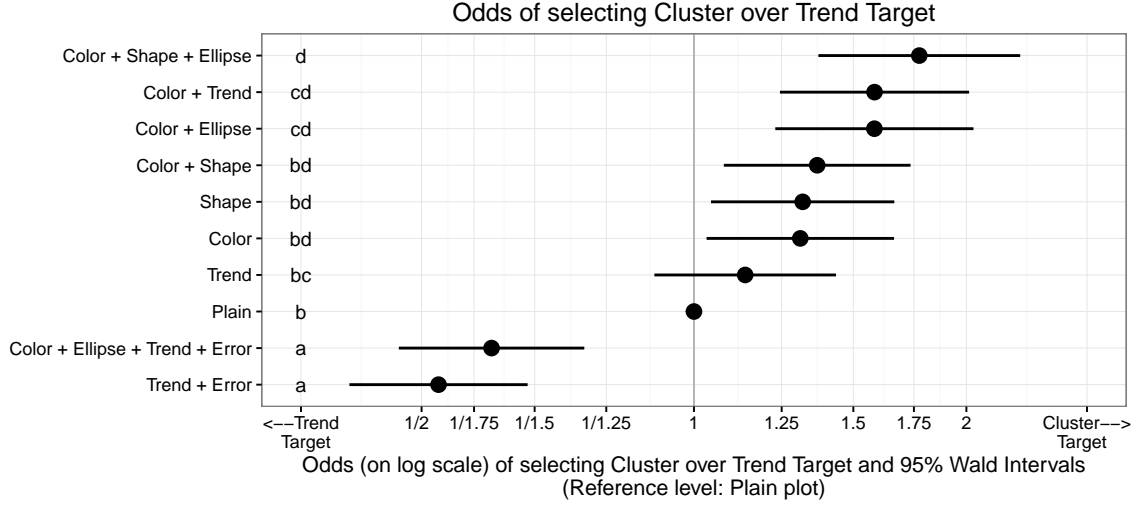


Figure 11: Estimated odds of decision for cluster versus trend target based on evaluations that resulted in the identification of one of these targets. Designs are significantly different if they do not share a letter as given on the left hand side of the plot.

Examining the model results from the perspective of Gestalt heuristics, it is clear that the similarity/proximity effect, as indicated by spatial clustering and aesthetics such as color and shape, dominates the equation, including dominating the color + trend (similarity vs. continuity) condition.

When trend line and prediction intervals (“error bands”, or “error” as an aesthetic description) are present in the same plot, the additional Gestalt principle of common region is recruited, in addition to the continuity heuristic present due to the trend line and the linear relationship between  $x$  and  $y$ . The interaction between these heuristics dominates the perceptual experience, decreasing the probability that a participant will select the cluster target plot in favor of the trend target.

This interaction effect explains the different outcomes seen by the two conditions with conflicting aesthetics: the color+trend condition is more likely to result in cluster plot selection, while the color + ellipse + trend + error condition is more likely to result in trend plot selection, because the combined effect of the gestalt heuristics present in the trend and prediction interval elements is stronger than the effect of color and ellipse elements, which only invoke Gestalt heuristics of similarity and common region.

In summary, the results from this experiment show that in order to gain a significant

difference from a plain representation and visually emphasize groups or trends, we need to make use of a statistical layer associated with a statistical interval/probability region in the form of an error band or an ellipse.

The lineup experimental protocol allows us to collect participant justifications for their target selection. These short explanations provide some additional insight into participant reasoning, and further support the gestalt explanation for the experimental results.

### 3.4 Participant Reasoning

As part of each trial, participants were asked to provide a short justification of their plot choice. Figure 12 gives an overview of summaries of participants’ reasoning in form of word clouds. In the word clouds, stopwords are excluded from participants’ reasons, unless they refer to quantities, such as ‘none’, ‘all’, ‘some’, ‘few’, etc. Reasons are also stemmed, so that words such as ‘group’, ‘groups’, ‘grouping’, ‘grouped’, and so on, all appear as the same (most prevalent) word in the cloud. What can be seen is a strong focus in terms of the reasoning depending on the outcome. If the participant chose one of the targets, the reasoning reflects this choice. When neither of the targets is chosen, there is less focus in the response. The word clouds look surprisingly similar independently of design - with the exception of the Ellipse + Color plot: here, the mentioning of specific colors is indicative of participants’ distraction from the intended target towards an imbalance of the color/cluster distribution.

Further examination of individual participants’ responses illustrates that group size (and thus, missing ellipses in the target plot) was a factor in the decision to identify specific null plots as different. Participants provided responses such as “There is no circle highlighting the yellow symbols in this plot” and “Lack of a circle around the red symbols”, which highlight the visual cues which were missing from the identified null plots.

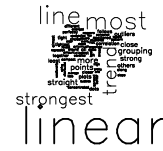
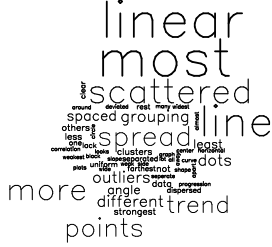
This was due to an unintended side-effect of using the k-means algorithm for cluster allocation in the null plots: due to an imbalance in the size of clusters, an additional cue was introduced into the null plots. The estimation of bounding ellipses fails for groups with fewer than three points and in these cases, ellipses were not drawn. Visually, the conspicuous absence of an ellipse led participants to select null plots with that feature.



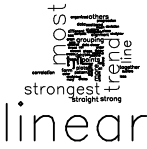
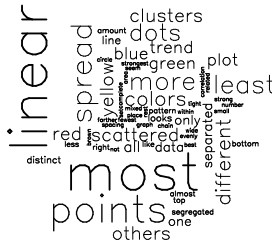
(a) Plain, neither target      (b) Plain, cluster target      (c) Plain, trend target



(d) Trend, neither target      (e) Trend, cluster target      (f) Trend, trend target



(g) Color, neither target      (h) Color, cluster target      (i) Color, trend target



(j) Color + Ellipse, neither      (k) Color + Ellipse, cluster      (l) Color + Ellipse, trend

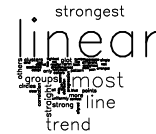
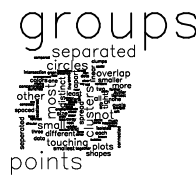
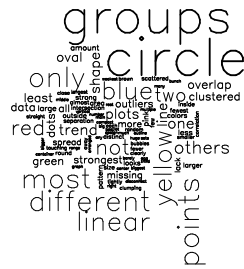


Figure 12: Wordclouds of participants' reasoning by outcome for a selected number of designs. Mostly, the reasoning and the choice of the target are highly associated. For the Color + Ellipse plot, participants were distracted from either target by an imbalance in the cluster/color distribution, as can be seen from the reasoning in the bottom left wordcloud.

When we include a variable encoding the absence of one of the ellipses in a lineup into model (3) it is highly significant ( $\chi^2_1=9.6$ ,  $P\text{-value}=0.002$ ), with an estimate of  $-0.8075$ , indicating that if one of the ellipses in a lineup is missing, the probability of picking the cluster target is reduced to less than half (44.6%) of the trend target. If we additionally consider the effect of a missing ellipse on individual designs, it is also significant ( $\chi^2_9=20.4$ ,  $P\text{-value}=0.0155$ ). Appendix section C.1 gives more details on this model and its effects.

## 4 Discussion and Conclusions

Taken together, the results presented suggest that plot aesthetics influence the perception of the dominant effect in the displayed data. This effect is not simply additive (otherwise, the two conflicting aesthetic conditions would result in similarly neutral effects); rather, the effect is consistent with layering of gestalt perceptual heuristics. Plot layers which add additional heuristics show larger effects than plot layers which duplicate heuristics that are already in play. For example, adding ellipses to a plot which has color aesthetics increases cluster recognition by recruiting the common region heuristic in addition to the point similarity heuristic recruited by color. Adding shape to a plot which has color aesthetics increases cluster recognition only slightly, but does not add additional gestalt heuristics (though point similarity is emphasized through two different mechanisms).

Statistically, this is important because the addition of ellipses or prediction intervals provides important statistical context, while reinforcing the visual emphasis by addition of the common region heuristic. Graphics which more effectively convey the statistical results are composed of aesthetic layers which recruit multiple gestalt heuristics in order to present a unified message. This represents a departure from the “show the data” mentality, but is still consistent with the goal of good graphics, that is, to convey the data in a way that is easily understandable while still providing appropriate detail.

While more studies are necessary to fully explore the nonadditive mechanism of additional gestalt heuristics and understand their effect in other types of plots, these results demonstrate the importance of carefully constructing graphs to convey the most important aspects of the displayed data.

# References

- Abdul-Rahman, A., Proctor, K. J., Duffy, B., and Chen, M. (2014), “Repeated Measures Design in Crowdsourcing-based Experiments for Visualization,” in *Proceedings of the Fifth Workshop on Beyond Time and Errors: Novel Evaluation Methods for Visualization*, New York, NY, USA: ACM, BELIV ’14, pp. 95–102.
- Adamo, S. H., Cain, M. S., and Mitroff, S. R. (2015), “Targets Need Their Own Personal Space: Effects of Clutter on Multiple-Target Search Accuracy,” *Perception*, 0301006615594921.
- Amazon (2010), “Mechanical Turk,” <https://www.mturk.com/mturk/welcome>.
- Ambady, N. and Rosenthal, R. (1993), “Half a minute: Predicting teacher evaluations from thin slices of nonverbal behavior and physical attractiveness,” *Journal of personality and social psychology*, 64, 431.
- Bobko, P. and Karren, R. (1979), “The perception of Pearson product moment correlations from bivariate scatterplots,” *Personnel Psychology*, 32, 313–325.
- Borgo, R., Abdul-Rahman, A., Mohamed, F., Grant, P. W., Reppa, I., Floridi, L., and Chen, M. (2012), “An empirical study on using visual embellishments in visualization,” *Visualization and Computer Graphics, IEEE Transactions on*, 18, 2759–2768.
- Buja, A., Cook, D., Hofmann, H., Lawrence, M., Lee, E.-K., Swayne, D. F., and Wickham, H. (2009), “Statistical inference for exploratory data analysis and model diagnostics,” *Philosophical Transactions of the Royal Society A: Mathematical, Physical and Engineering Sciences*, 367, 4361–4383.
- Cain, M. S., Dunsmoor, J. E., LaBar, K. S., and Mitroff, S. R. (2011), “Anticipatory anxiety hinders detection of a second target in dual-target search,” *Psychological Science*, 22, 866–871.
- Cleveland, W. S. (1994), *The Elements of Graphing Data*, Hobart Press, 1st ed.

- Cleveland, W. S. and McGill, R. (1984), “Graphical Perception: Theory, Experimentation, and Application to the Development of Graphical Methods,” *Journal of the American Statistical Association*, 79, pp. 531–554.
- Curhan, J. R. and Pentland, A. (2007), “Thin slices of negotiation: predicting outcomes from conversational dynamics within the first 5 minutes.” *Journal of Applied Psychology*, 92, 802.
- Demiralp, C., Bernstein, M., and Heer, J. (2014), “Learning Perceptual Kernels for Visualization Design,” *Visualization and Computer Graphics, IEEE Transactions on*, 20, 1933–1942.
- DeMita, M. A., Johnson, J. H., and Hansen, K. E. (1981), “The validity of a computerized visual searching task as an indicator of brain damage,” *Behavior Research Methods & Instrumentation*, 13, 592–594.
- Few, S. (2009), *Now You See It: Simple Visualization Techniques for Quantitative Analysis*, Burlingame, CA: Analytics Press, 1st ed.
- Fleck, M. S., Samei, E., and Mitroff, S. R. (2010), “Generalized satisfaction of search: Adverse influences on dual-target search accuracy.” *Journal of Experimental Psychology: Applied*, 16, 60.
- Gegenfurtner, K. R. and Sharpe, L. T. (2001), *Color vision: From genes to perception*, Cambridge University Press.
- Gladwell, M. (2007), *Blink: The power of thinking without thinking*, Back Bay Books.
- Goldstein, E. B. (2009), *Encyclopedia of perception*, Sage Publications.
- Hanrahan, P. (2003), “Tableau software white paper - visual thinking for business intelligence,” *Tableau Software, Seattle, WA*.
- Healey, C. G., Booth, K. S., and Enns, J. T. (1996), “High-speed visual estimation using preattentive processing,” *ACM Transactions on Computer-Human Interaction (TOCHI)*, 3, 107–135.

- Healey, C. G. and Enns, J. T. (1999), “Large datasets at a glance: Combining textures and colors in scientific visualization,” *Visualization and Computer Graphics, IEEE Transactions on*, 5, 145–167.
- Hofmann, H., Follett, L., Majumder, M., and Cook, D. (2012), “Graphical tests for power comparison of competing designs,” *Visualization and Computer Graphics, IEEE Transactions on*, 18, 2441–2448.
- Hogarth, R. M. (2014), “Deciding Analytically or Trusting Your Intuition? The Advantages and Disadvantages of Analytic and Intuitive Thought,” *The Routines of Decision Making*, 67.
- Lewandowsky, S. and Spence, I. (1989a), “Discriminating strata in scatterplots,” *Journal of the American Statistical Association*, 84, 682–688.
- (1989b), “The perception of statistical graphs,” *Sociological Methods & Research*, 18, 200–242.
- Majumder, M., Hofmann, H., and Cook, D. (2013), “Validation of visual statistical inference, applied to linear models,” *Journal of the American Statistical Association*, 108, 942–956.
- (2014), “Human Factors Influencing Visual Statistical Inference,” .
- Mosteller, F., Siegel, A. F., Trapido, E., and Youtz, C. (1981), “Eye fitting straight lines,” *The American Statistician*, 35, 150–152.
- Piepho, H.-P. (2004), “An algorithm for a letter-based representation of all-pairwise comparisons,” *Journal of Computational and Graphical Statistics*, 13, 456–466.
- Robinson, H. (2003), “Usability of Scatter Plot Symbols,” *ASA Statistical Computing & Graphics Newsletter*, 14, 9–14.
- Roy Chowdhury, N., Cook, D., Hofmann, H., Majumder, M., and Zhao, Y. (2014), “Utilizing Distance Metrics on Lineups to Examine What People Read From Data Plots,” *arXiv.org*.

- Scaife, M. and Rogers, Y. (1996), “External cognition: how do graphical representations work?” *International journal of human-computer studies*, 45, 185–213.
- Spence, I. and Garrison, R. F. (1993), “A remarkable scatterplot,” *The American Statistician*, 47, 12–19.
- Treisman, A. (1985), “Preattentive processing in vision,” *Computer Vision, Graphics, and Image Processing*, 31, 156 – 177.
- Treisman, A. M. and Gelade, G. (1980), “A feature-integration theory of attention,” *Cognitive psychology*, 12, 97–136.
- Tukey, J. W. (1977), *Exploratory Data Analysis*, Lebanon, IN: Addison Wesley.
- Vanderplas, S. and Hofmann, H. (2016), “Spatial Reasoning and Data Displays,” *IEEE Transactions on Visualization and Computer Graphics*, 459–468.
- Wickham, H., Cook, D., Hofmann, H., and Buja, A. (2010), “Graphical inference for infovis,” *Visualization and Computer Graphics, IEEE Transactions on*, 16, 973–979.
- Zhang, J. (1997), “The nature of external representations in problem solving,” *Cognitive science*, 21, 179–217.

## A Simulation Study of the Parameter Space

Using 1000 simulations for each of the 98 combinations of parameters ( $K = \{3, 5\}$ ,  $\sigma_C = \{.1, .15, .2, .25, .3, .35, .4\}$ ,  $\sigma_T = \{.2, .25, .3, .35, .4, .45, .5\}$ ), we explored the effect of parameter value on the distribution of summary statistics describing the strength of the linear relationship ( $R^2$ ) and cluster strength for null and target plots.

Figures 13a and 13b show the 25th and 75th percentiles of the distribution of  $R^2$  and cluster strength summary statistics for each set of parameter values. These plots guide our evaluation of “easy”, “medium” and “hard” parameter values for trend and cluster tasks.

Additionally, we note that there is an interaction between  $\sigma_C$  and  $\sigma_T$ : the distinction between target and null on a fixed setting of clustering becomes increasingly difficult as the standard deviation for the linear trend is increased, and vice versa. There may additionally be a three-way interaction between  $\sigma_C$ ,  $\sigma_T$ , and  $K$ : the width of the blue intervals (bottom figure) changes between different levels of  $K$  and for different levels of  $\sigma_C$  and  $\sigma_T$ . These interactions suggest that in order to examine differences in aesthetics, we must block by parameter settings (this can be accomplished through blocking by dataset). Each dataset is non-deterministic, because we have a random process generating from different parameter settings, not a deterministic run setting as in an engineering setting. It is thus important to use replicates of each parameter setting to ensure that we can separate data-level effects from parameter-level effects.

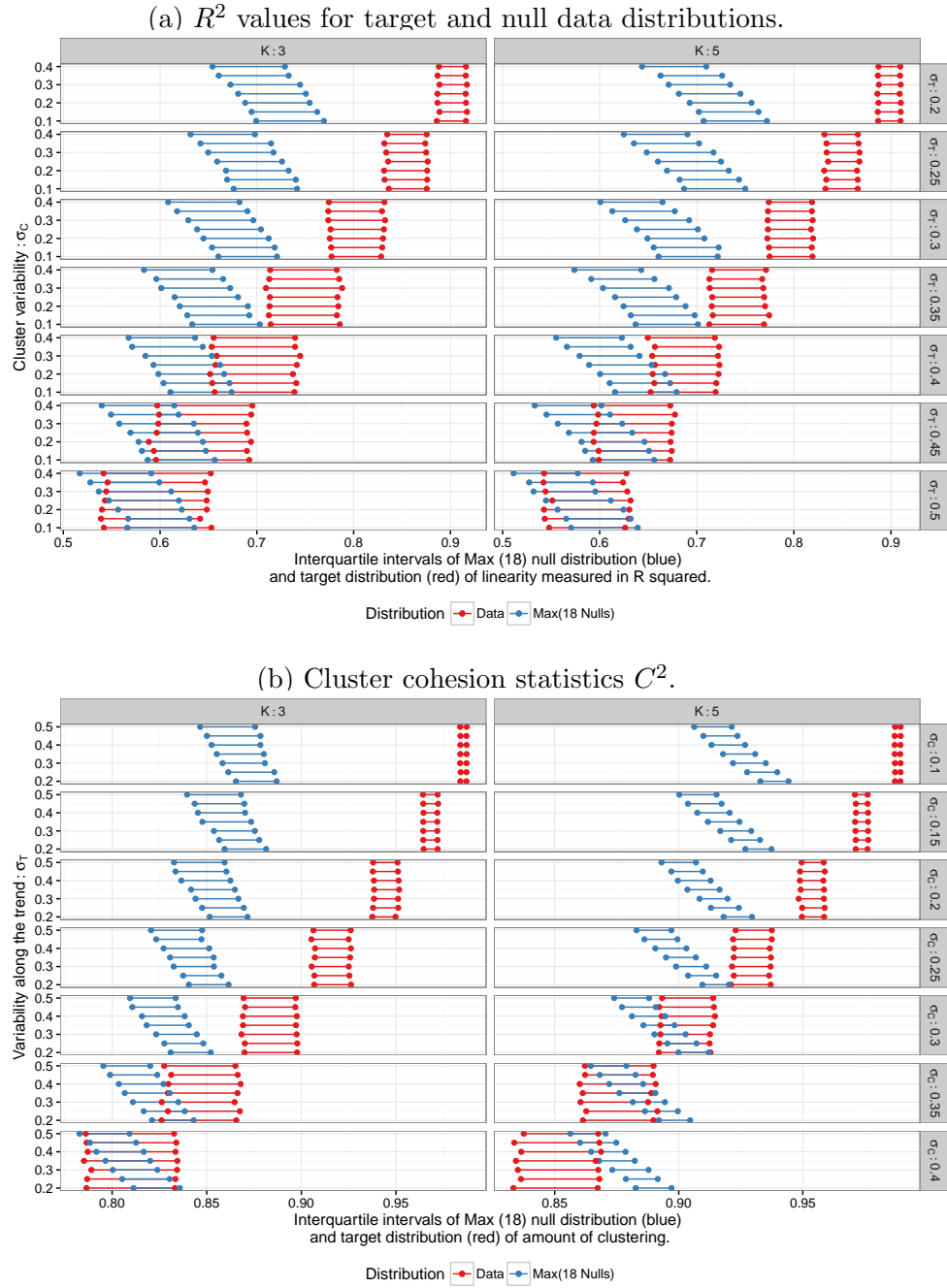


Figure 13: Simulated interquartile ranges between target and most extreme statistic from one of the 18 null plots.



## B Simulation based inference in a two-target lineup scenario

Assume that there are two targets embedded in a lineup of overall size  $m$ , where  $m$  in our experiment is taken to be  $m = 20$ . Let  $A$  be the event that one of these targets is chosen. Under the null hypothesis that both targets are consistent with being created based on data from the null model, we can assume that under the null hypothesis the expected value of the probability that an observer picks one of these plots from the lineup is  $2/m = E[P(A \mid H_o)]$ . For the distribution of  $A \mid H_o$  we employ a simulation-based strategy: Under the null hypothesis, we can assume, that the  $p$ -value corresponding to a hypothesis test ‘the presented data is consistent with the null model’ has a standard uniform distribution, i.e.  $p_i \sim U[0, 1]$  i.i.d. for all  $1 \leq i \leq m$ . We assume that the choice observers make can be modeled using a multinomial distribution, where the probability  $\pi_i$  to pick panel  $i$  is inversely linear to  $p_i$ , with  $\sum_{i=1}^m \pi_i = 1$ .

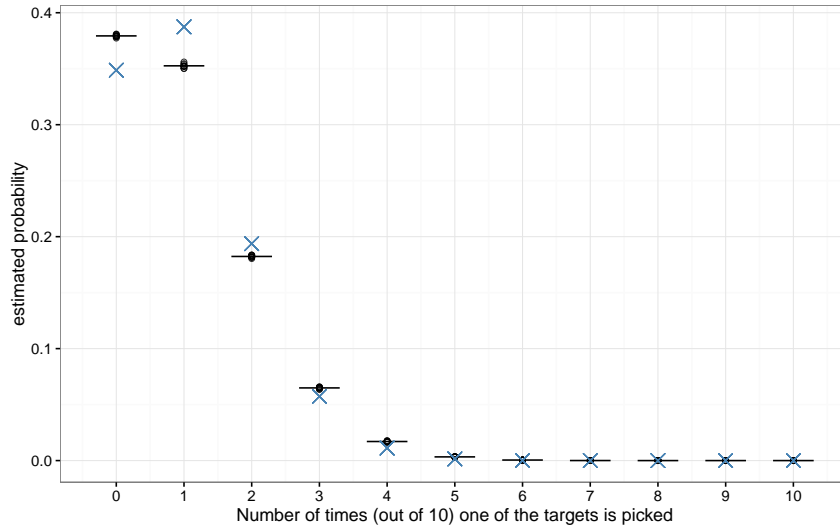


Figure 14: Ten simulations of size  $b_2 = 1,000$  and  $b_1 = 100$  for lineups of size  $m = 20$  assuming  $K = 10$  evaluations. The averages of the ten simulation runs are shown as lines. The crosses are probabilities from Binomial  $B_{2/20, 10}$ .

W.l.o.g. we can assume that the two target plots are in positions 1 and 2. Given that a lineup was evaluated by  $K$  individuals, the simulation process for the conditional probability of identifying one of the targets given that both are consistent with the null

model,  $P(A|H_o)$ , is then as follows:

1. Pick two values  $p_i \sim U[0, 1], i = 1, 2$ .
2. Repeat  $b_1$  times:
  - (a) Pick  $m - 2$  values  $p_i \sim U[0, 1], i = 3, \dots, m$ .
  - (b) Pick  $K$  values from a Multinomial distribution with  $\pi = \frac{1-p}{\|1-p\|}$ , i.e.  $x_j \sim M_\pi, i = 1, \dots, K$
  - (c) Return the number of times that  $x_j$  is 1 or 2.

Repeat the above process  $b_2$  times, and average results for a distribution of  $A | H_o$ . The choice of  $b_1$  and  $b_2$  decides on the number of decimal places to which the estimated distribution can be used reliably.

Figure 14 shows the result of this simulation approach for a lineup of size 20 assuming  $K = 10$  evaluation. The density of  $A | H_o$  is plotted for ten runs (open circles). The variability in the results is relatively small - for comparison, the density of a Binomial distribution  $B_{2/20,10}$  is shown using crosses. The main difference between the densities is the probability of zero or only one identification, while the tail probabilities are very similar.

## C Modelling results

We are discussing four main models in this section. According to its dependent variables, these models are:

**Accuracy (in section C.1):** a lineup is considered to be evaluated ‘accurately’, if at least one of its two targets is identified in an evaluation. We model this probability, i.e.  $P(C_{ijk} \cup T_{ijk})$ , where  $C_{ijk}$  and  $T_{ijk}$  are binary variables describing the events that participant  $k$  identifies the cluster/trend target in dataset  $j$  presented with design  $i$ .

**Response time (in section C.2):** response time is measured as the time between which a lineup is presented to a participant and the time point at which an answer is submitted. On average, participants need 40 seconds to respond to a lineup. Factors

that affect this average (including accuracy, confidence level, and user justification) are also investigated.

**Confidence (in section C.3):** for each lineup, participants are asked to provide a subjective evaluation of the level of confidence they have in the choice they made, in the form of an integer value between 0 (least) to 5 (highest).

**Balance between targets (in section C.4):** because each lineup includes two targets, we can compare the frequency of identification of each target type. The objective here is to model the conditional probability of a cluster target identification given one of the two targets was identified, i.e. we want to model  $P(C_{ijk} | C_{ijk} \cup T_{ijk})$ .

The parameter estimation for the first three models is based on all 12010 available lineup evaluations, while the last model is based on only those lineups where at least one of the targets was identified. An overview of all of the fixed effects considered for each one of these models is given in Table 3. All models are fitted using the same random effects structure: we assumed one random effect for dataset specific characteristics, one random effect to account for individuals' different skills, and a random error term. We are assuming that all random effects are normally distributed and pairwise orthogonal.

The general model structure we are using for all four main models is the following:

$$g(E[Y]) = \mathbf{W}\alpha + \mathbf{X}\beta + \mathbf{J}\gamma + \mathbf{K}\eta, \quad (4)$$

where

$g(\cdot)$ , the left hand side, is made up of a link function  $g$  that connects the (conditional) expected value of dependent variable  $Y$  to the structural right hand side. We further assume that  $Y = g^{-1}(\cdot) + \epsilon$ , with  $\epsilon \stackrel{\text{approx}}{\sim} N(0, \sigma^2 I_{n \times n})$ .

$\alpha, \beta$  are vectors of fixed effects, where  $\beta$  is a vector corresponding to the ten designs investigated, and  $\alpha$  encompasses all 'other' fixed effects that might have an effect on the dependent variable besides the design of a plot,

$W, X$  are the design matrices corresponding to the fixed effects,

		Model			
Dependent Variable		Face-off C.4	Accuracy C.1	Response Time C.2	Confidence C.3
Transformation		(logit)	(logit)	(log)	—
Effect	Parameter				
Design	$\beta$	✓	✓	✓	✓
Within cluster variability	$\alpha_C$	✓	✓	✓	✓
Variability around trendline	$\alpha_T$	✓	✓	✓	✓
Number of clusters	$\alpha_K$	✓		✓	✓
First trial	$\alpha_1$			✓	✓
Lineup order	$\alpha_O$		✓	✓	✓
(log) Response time	$\tau$		✓	—	✓
Gini impurity	$\gamma$		✓		
Single missing ellipse	$\nu$	✓			
Target type (cluster, trend, neither, both)	$\omega_{\{C,T,N,B\}}$	—	—	✓	✓
Data		identified targets	all evaluations	all evaluations	all evaluations

Table 3: Overview of all models and their respective fixed effects. The same random effects were used for each model. All effects were investigated if applicable (otherwise marked by ‘—’). Checkmarks indicate significance at the 0.05 level.

$\gamma_j \stackrel{iid}{\sim} N(0, \sigma_{\text{data}}^2)$ , random effect for dataset specific characteristics,

$\eta_k \stackrel{iid}{\sim} N(0, \sigma_{\text{participant}}^2)$ , random effect for participant characteristics.

We also assume that random effects for dataset and participant are orthogonal.

## C.1 Accuracy Model

The lineup protocol provides an easy way of measuring accuracy of evaluations by assessing the number of participants who identified the data plot. In the modified version, we can use this as well by regarding any lineup evaluation resulting in an identification of at least one of the two targets as ‘accurate’. We therefore want to model the probability that participant  $k$  identifies (at least) one of the targets on the lineup (using aesthetics set  $i$ ) of dataset  $j$ ,  $P(C_{ijk} \cup T_{ijk})$ . We use the logit function as the link function  $g(\cdot)$ .

The vector  $\alpha$  of fixed effects consists of  $(\mu, \alpha_T, \alpha_C, \alpha_K, \alpha_O)$ , where

$\mu$  is an average baseline accuracy (and should not be interpreted, because all other effects are assumed to be zero, which is not practically possible),

$\alpha_C, \alpha_T$  are the average effects of the standard error around trend lines  $s_T \in \{0.25, 0.35, 0.45\}$  and clusters  $s_C \in \{0.2, 0.25, 0.3, 0.35\}$  on accuracy,

$\alpha_K$  is the effect of the number of clusters  $K \in \{3, 5\}$ , and

$\alpha_O$  is an order effect, i.e. an effect on accuracy for successive lineups.

Table 4 shows an overview of the parameters of the accuracy model and their estimates. Both  $\alpha_T$  and  $\alpha_C$  have large negative effects that are highly significant. This indicates that as the signal in the target plots weakens (by an increase in variability around the trend line or within cluster variability), accuracy of participants decreases on average.  $\alpha_K$  has a small negative effect, i.e. participants are on average answering lineups with three clusters with more accuracy than lineups with five clusters. However, this effect is not significant. The order effect  $\alpha_O$  is small, but significant; as participants answer more lineups, their accuracy decreases on average by about 2% for each additional evaluation

$\alpha_O$  may represent a fatigue effect or an experience effect. Fatigue effects have been documented (Abdul-Rahman et al., 2014) in studies where participants complete several trials which are similar in a short period of time. It is also possible that as participants completed additional trials, they learned to look for certain cues (e.g. number of groups) which led to the selection of plots which had large differences in group size. While this approach is reasonable using inductive logic, participants using this strategy would be less likely to select the cluster or trend targets as a result.

As the lineups in this study were randomly ordered, either hypothesized effect is unlikely to bias the estimates for dataset and aesthetic effects. In future experiments, it may be advantageous to utilize a two-part experimental design or add a short break to mitigate both potential fatigue and learning effects.

We additionally investigate two more effects: (log) response time and the effect of imbalances in the group allocation on accuracy.

### C.1.1 Effect of response time

The effect of (log) response times on accuracy is highly significant ( $\chi^2_1=80.7$ ,  $P\text{-value}<0.0001$ ). With each unit increase in (log) response time the probability for a target identi-

	Parameter	Estimate	Std. Error	$z$ -value	$\Pr(> z )$
	$\mu$	6.47	1.08	6.01	$< 0.0001$
	$\alpha_T$	-2.55	1.20	-2.12	0.0339
	$\alpha_C$	-8.59	2.40	-3.58	0.0003
	$\alpha_K$	-0.11	0.11	-0.93	0.3523
	$\alpha_O$	-0.02	0.01	-2.33	0.0199
<b>Design</b>	$\beta$				
	Plain	0.00	—	—	—
	Trend + Error	-0.08	0.14	-0.57	0.5701
	Shape	-0.08	0.14	-0.57	0.5694
	Trend	-0.35	0.13	-2.61	0.0090
	Color + Shape	-0.51	0.13	-3.95	0.0001
	Color	-0.60	0.13	-4.64	$< 0.0001$
	Color + Trend	-0.70	0.13	-5.49	$< 0.0001$
	Color + Ellipse + Trend + Error	-1.12	0.12	-9.05	$< 0.0001$
	Color + Shape + Ellipse	-1.40	0.12	-11.45	$< 0.0001$
	Color + Ellipse	-1.47	0.12	-12.09	$< 0.0001$

Table 4: Parameters and estimates of the accuracy model.

fication is reduced on average by about  $1/3$ . However, in the long run, a secondary effect takes place, and response time has a positive effect on accuracy again. Fitting an additional quadratic term in the model is also highly significant ( $\chi_1^2=13.3$ ,  $P$ -value= $3 \times 10^{-4}$ ), and leads to an overall minimum accuracy over time at a response time of about 150 seconds.

This speed/accuracy relationship is more complicated than the typical speed/accuracy tradeoff, which assumes that accuracy increases with decreasing speed. Instead, when evaluating lineups, two effects seem to compete: Initially, participants may be able to fairly quickly (and accurately) select the target plot using high-bandwidth visual differences between the plots. If this initial strategy fails, participants may begin making pairwise comparisons in an attempt to select between one of several potential “targets”. These comparisons are slow, but eventually participants may succeed in using inductive reasoning to identify the target plot, producing a slow increase in accuracy after about 150 seconds.

The accuracy of initial impressions made with relatively little information has been documented in the popular press (Gladwell, 2007) and in scholarly literature (Curhan and Pentland, 2007; Ambady and Rosenthal, 1993; Hogarth, 2014). Participants who select a target quickly are likely utilizing intuition as well as conscious reasoning; when combined with lineups which have a clear signal, this approach is fairly accurate. When intuition and initial approaches fail, however, participants must resort to a slower, deliberate approach which may include attempting to determine both the evaluation metric to utilize and the most different plot when utilizing that metric. This process would take more time and have a higher error rate, particularly if the participant uses a strategy which is not aligned with the data-generating model (for instance, evaluating the size of the groups rather than the spatial clustering of points). The combination of these two effects could explain the quadratic speed/accuracy relationship seen in this model.

Goldilocks lineups - easy, medium, hard - which can be solved using the intuitive or inductive approaches.

### C.1.2 Effect of group imbalances

Gini impurity measures the homogeneity of group allocations. Let  $n_i$  be the number of elements in the  $i$ th cluster,  $i = 1, \dots, K$ , with  $n = \sum_{i=1}^K n_i$  and let  $p_i = n_i/n$  be the

frequency of cluster  $i$ . Then the gini impurity is calculated as

$$G(p_1, \dots, p_K) = \frac{K}{K-1} \sum_{i=1}^K p_i(1 - p_i).$$

$G$  is an index between 0 and 1, where 0 is maximum diversity - in the sense, that there is only one group present, i.e.  $p_i = 0$  for all but one of the groups. A Gini impurity of 1 indicates perfect homogeneity, i.e.  $p_i = 1/K$  for all  $i$ .

The probability of picking at least one of the targets significantly increases with an increase in Gini impurity, that is, with more equal group sizes ( $\chi_1^2=5.9$ ,  $P$ -value=0.0153).

In other words, a small Gini index indicates the presence of a null plot with large differences in the number of elements in each group. This served as a(n unintended) distractor away from the intended targets and therefore led to a drop in accuracy. Different designs are affected differently strong (two-way interaction:  $\chi_9^2=34.7$ ,  $P$ -value  $< 0.0001$ ): Plots making use of color are all affected more strongly by deviations from homogeneity than plots without color. If ellipses are drawn, the effect becomes even more pronounced. Figure 15 gives an overview of the relationship between predicted accuracy and designs for levels of homogeneity between 0.5 and 1 (similar to the range of Gini impurity observed in the study).

Other features measuring the imbalance within a lineup that we considered besides Gini impurity are

- the difference between the maximum and the minimum number of elements in each of the groups of a lineup, and
- the number of ellipses missing from the lineup.

The range of group sizes does not have a significant effect on the probability to pick at least one of the targets, even if different designs are taken into account. Similarly, a single absent ellipse does not lead to a significant change in the probability of detecting one of the target plots. Neither the number of missing ellipses nor the absence of at least one ellipse have a significant effect on this probability, not even when we consider the impact of individual designs.



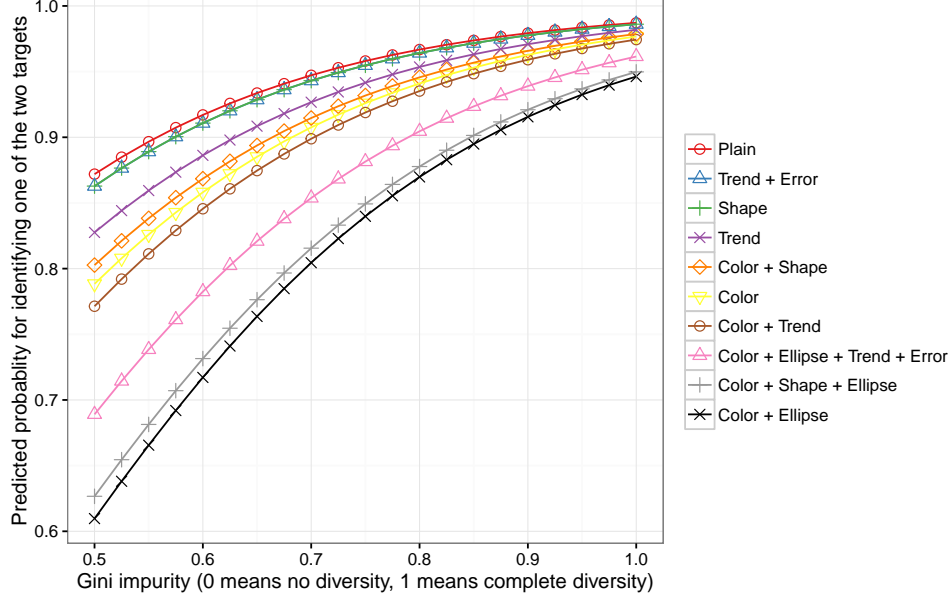


Figure 15: Predicted accuracy values for designs given different values of the gini impurity measure. Values of gini impurity between 0.59 and 1 were actually observed in the panels of the lineups. Accuracy of all designs with color are lower than their non-colored counterparts, and the addition of ellipses further decreases accuracy. With a large deviation from equi-distributed groups, accuracy is disproportionately affected when color or ellipse aesthetics are present.

These features have also been included in the faceoff model of section C.4 to investigate whether group size imbalance or missing ellipses affects the probability of selecting one target over the other.

## C.2 Modelling response times

While we do not have the same amount of control in an AMT study that we would have in a lab setting, we can accurately capture the time between presenting a lineup to a participant and the time at which results are submitted. A histogram of these times is given in Figure 16. Response times are extremely skew. In the model we therefore use the log of response times  $T = (t_{ijk})_{n \times 1}$  as the dependent variable.

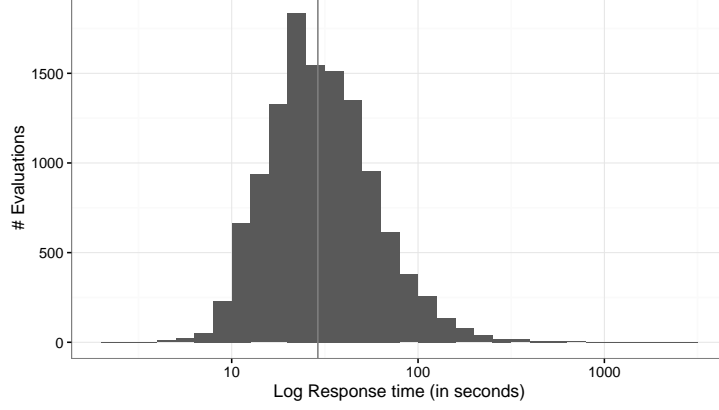


Figure 16: Histogram of (log) response times. The median evaluation time (vertical line) is 29 seconds.

For the vector of fixed effects,  $\alpha$ , we estimate, as before, the effects of variability ( $\alpha_C$  and  $\alpha_T$ ) on response times, as well as the number of clusters shown ( $\alpha_K$ ). Aside from this, we also consider the average effect of the first trial,  $\alpha_1$ , and the effect of successive trials,  $\alpha_O$ , on the response time.  $\omega_C, \omega_T, \omega_B$ , and  $\omega_N$  is a set of parameters assessing the effect of the outcome of the lineup evaluation on response time (the letters in the subscript stand for ‘C’luster, ‘T’rend, ‘B’oth, and ‘N’one).

Table 5 gives an overview of all parameters of the response time model and their estimates. Similar to what has been found in other lineup studies (Majumder et al., 2014; Hofmann et al., 2012), participants take on average 25% longer to respond to the first lineup than to subsequent lineups. Aside from this, we see that as the difficulty of lineups increases (controlled by an increase in the parameters  $s_C$  and  $s_T$ ), the average amount of time participants spend on each evaluation significantly increases.

On average, participants respond to each successive lineup about 3% faster.

Depending on the outcome of the evaluation, there are differences in the amount of time: if either one of the targets is identified, the amount of time taken to answer is significantly shorter than if neither of the targets is found. Answers take on average the longest, if both targets are identified (however, this only happens in 0.6% of the responses). Plot aesthetics have a significant impact on the amount of time for responses, with increasing plot complexity associated with increased evaluation time. This may be a function of

increased cognitive load, as participants must examine more features in order to identify which plot has the strongest signal. For instance, when color, ellipses, trend lines, and error bands are present, participants have to compare the allocation of color to points, the size, shape, and distance between each set of ellipses, the slope of each trend line, and the width of the error bands. While each participant almost certainly does not complete a full pairwise comparison of all 20 lineup plots across each feature set, the increased complexity of each additional feature does increase the space which must be examined using perceptual heuristics in order to identify the target plot correctly. This is consistent with Borgo et al. (2012), who found that visual embellishments increase the time required to perform visual search tasks using data displays.

### C.3 Model of confidence levels

With each lineup evaluation, participants were asked to give feedback on their level of confidence from 0 (least) to 5 (most). As an approximation, we can fit a mixed effects model with this variable as the dependent, and investigate its relationship with the parameters controlling difficulty of a lineup, the time taken to evaluate the lineup and its outcome.

The approximation of confidence level (which is a bounded, discrete variable) by a normal distribution is far from perfect, but the results are very interpretable.

The vector of fixed effects,  $\alpha$ , includes besides the previously described effects of the control parameters  $\alpha_C, \alpha_T, \alpha_K$ , the effects of lineup order  $\alpha_1, \alpha_O$ , the effect of evaluation outcome  $\omega_C, \omega_T, \omega_B, \omega_N$ , also parameters that control for the amount of time taken by participants to evaluate a lineup:  $\tau$  is the effect of log response time on the level of confidence reported by a participant.

Table 6 gives an overview of the parameters and estimates of the model.

Over the course of the study, confidence deteriorates with each additional lineup by about 0.03 (while significant, this effect on confidence is fairly small, as confidence is measured on a scale of 0 to 5). Beyond this order effect, the first trial does not have a significant effect on the reported confidence.

The longer a participant needs to evaluate a lineup, the lower on average will be the value of confidence reported along with it. Similarly, an increase in lineup difficulty (as

	Parameter	Estimate	Std. Error	$z$ value	$P$ -value
	$\mu$	2.664	0.108	24.559	< 0.0001
	$\alpha_{K=3}$	0.000	—	—	—
	$\alpha_{K=5}$	0.124	0.029	4.297	< 0.0001
	$\alpha_T$	0.481	0.153	3.152	< 0.0001
	$\alpha_C$	1.664	0.302	5.503	< 0.0001
	$\alpha_1$	0.084	0.016	5.133	< 0.0001
	$\alpha_O$	-0.030	0.002	-17.273	< 0.0001
<b>Outcome</b> $\omega$	Trend	0.000	—	—	—
	Cluster	0.027	0.013	2.117	0.0342
	Neither	0.181	0.015	11.736	< 0.0001
	Both	0.347	0.057	6.079	< 0.0001
<b>Design</b> $\beta$	Plain	0.000	—	—	—
	Shape	0.110	0.019	5.903	< 0.0001
	Color	0.130	0.019	6.961	< 0.0001
	Trend	0.144	0.019	7.714	< 0.0001
	Trend + Error	0.163	0.019	8.725	< 0.0001
	Color + Ellipse	0.206	0.019	10.895	< 0.0001
	Color + Shape	0.209	0.019	11.194	< 0.0001
	Color + Trend	0.215	0.019	11.469	< 0.0001
	Color + Shape + Ellipse	0.203	0.019	10.752	< 0.0001
	Color + Ellipse + Trend + Error	0.248	0.019	13.187	< 0.0001

Table 5: Model parameters and estimates for (log) response time in seconds. The  $P$ -values are based on a normal approximation of the  $t$  statistics.

controlled by increased values of  $s_C$  and  $s_T$ ) goes hand in hand with a significant decrease in confidence. If neither one or both of the two targets were identified, the reported confidence level is significantly lower than if one of the two targets was identified<sup>1</sup>. Aesthetics in general

<sup>1</sup>The decrease in confidence when both targets are identified may be due to the additional complexity of dual-target search (Fleck et al., 2010; Cain et al., 2011; Adamo et al., 2015)

did not have a significant effect on confidence levels. However, individual aesthetics did lead to a significant increase in confidence: any plot showing ellipses increases the level of confidence on average by about 0.1. These results suggest that the speed of evaluation is not significantly contributing to shifting the balance between selecting one target over the other.

	Parameter	Estimate	Std. Error	$z$ -value	$P$ -value
	$\mu$	5.898	0.147	40.044	< 0.0001
	$\alpha_O$	-0.033	0.003	-10.738	< 0.0001
	$\alpha_1$	0.002	0.029	0.083	0.9336
	$\tau$	-0.295	0.016	-18.507	< 0.0001
	$\alpha_T$	-0.538	0.198	-2.719	0.0066
	$\alpha_C$	-1.899	0.389	-4.879	< 0.0001
	$\alpha_{K=3}$	0.000	—	—	—
	$\alpha_{K=5}$	-0.131	0.037	-3.559	0.0004
<b>Outcome</b> $\omega$	Trend	0.000	—	—	—
	Cluster	-0.028	0.022	-1.263	0.2065
	Both	-0.213	0.102	-2.084	0.0372
	Neither	-0.220	0.028	-7.971	< 0.0001
<b>Design</b> $\beta$	Shape	-0.006	0.034	-0.187	0.8518
	Plain	0.000	—	—	—
	Color + Shape	0.024	0.034	0.698	0.4855
	Color	0.040	0.034	1.178	0.2390
	Trend	0.050	0.034	1.497	0.1343
	Trend + Error	0.052	0.034	1.533	0.1252
	Color + Trend	0.058	0.034	1.707	0.0878
	Color + Ellipse	0.068	0.034	1.997	0.0459
	Color + Ellipse + Trend + Error	0.106	0.034	3.132	0.0017
	Color + Shape + Ellipse	0.107	0.034	3.156	0.0016

Table 6: Parameters and estimates for the model of participants' confidence.

## C.4 Faceoff Model

Figures 17 and 18 show the proportion of outcomes for either the cluster target, the trend target, both or none of them. Overall, cluster targets are picked more often than trend targets. For very small residual errors around the line fit and large within-cluster errors, the number of line target picks are highest. As the standard error around the trend line increases, the number of times the corresponding target is picked decreases. Similarly, an increase in within-cluster error is associated with a decrease of the number of cluster target picks. The effect of the different designs is consistent across different parameter settings (the order of plot designs is given by the marginal effects as estimated in the faceoff model. Numerical estimates can be found in Table 7). The effect of designs is most pronounced, when the ambiguity between the two targets is strong, i.e. close to a 50:50 decision between the targets. In those cases the additional aesthetics tip the balance in favor of one target over the other.

Response time (composed of log(response time) and effect of first trial) does not have a significant effect on the decision between cluster and trend target ( $\chi^2_2=4.5$ ,  $P$ -value=0.1067). Nor does the confidence level of participants ( $\chi^2_5=4.6$ ,  $P$ -value=0.4716).

What does have a significant effect on the balance between cluster target and trend target is the absence of one of the ellipses in one of the panels of the lineup: a single missing ellipse (that is, a group size of less than 4) cuts the probability that the cluster target is selected by more than half (44.6%;  $\chi^2_1=9.6$ ,  $P$ -value=0.002). We also find a significant effect if we additionally take the two-way interaction between a single missing ellipse and individual designs into account ( $\chi^2_9=20.4$ ,  $P$ -value=0.0155). These effects are summarised in Figure 19.

	Parameter	Log Odds Ratio	95% Lower	95% Upper
	Intercept	1.018	-1.615	3.651
	$\alpha_T$	16.254	13.276	19.231
	$\alpha_C$	-16.038	-21.935	-10.140
	$\alpha_K$	-0.281	-0.563	0.001
<b>Design</b>	$\beta$ Trend + Error	-0.650	-0.877	-0.423
	Color + Ellipse + Trend + Error	-0.515	-0.751	-0.279
	Plain	0.000	—	—
	Trend	0.130	-0.101	0.361
	Color	0.271	0.032	0.509
	Shape	0.277	0.043	0.510
	Color + Shape	0.314	0.076	0.551
	Color + Ellipse	0.459	0.207	0.711
	Color + Trend	0.459	0.219	0.700
	Color + Shape + Ellipse	0.573	0.317	0.830

Table 7: Odds Ratios of picking the cluster target over the trend target (with the plain design as a baseline). The last two columns are 95% confidence intervals. Within the plain plots, the odds of choosing the cluster target over the trend target is about 2:1.

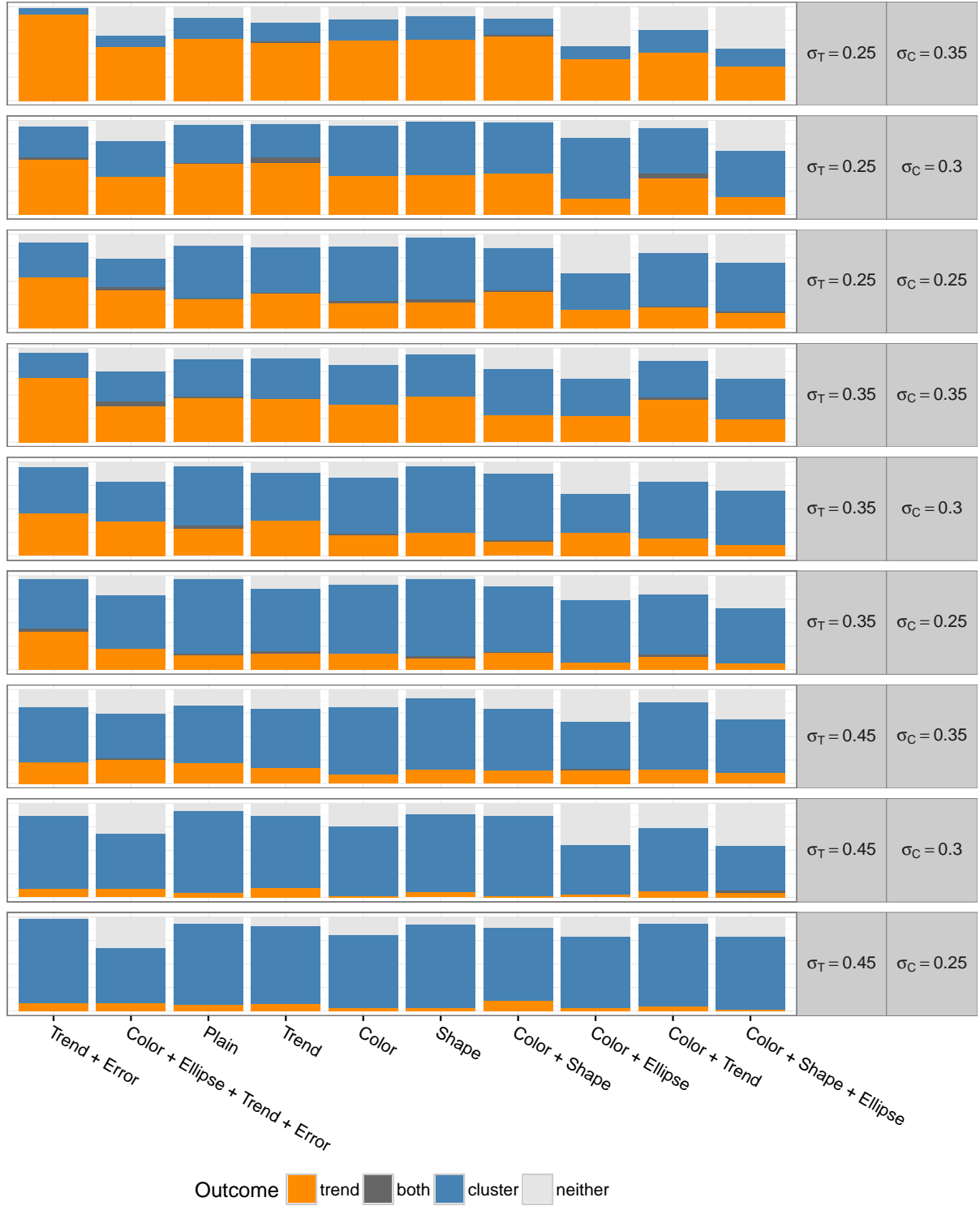


Figure 17: Outcome by design and parameter setting for lineups with trend and cluster targets. The cluster target consists of  $K = 3$  clusters.





Figure 18: Outcome by design and parameter setting for lineups with trend and cluster targets. The cluster target consists of  $K = 5$  clusters.

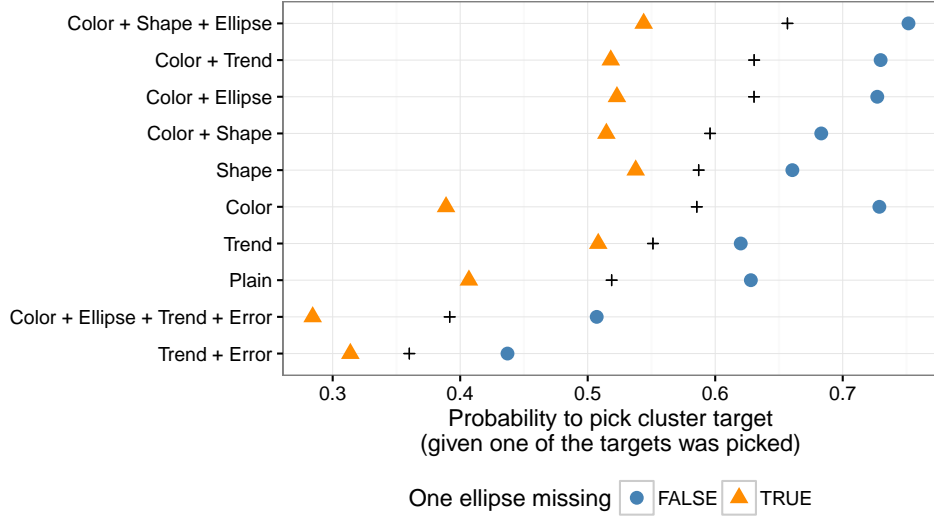


Figure 19: Overview of the probability to pick the cluster target given the different designs.  $s_C$  and  $s_T$  are set to 0.25 and 0.275, respectively, and  $K = 3$  is assumed. The plus symbols indicate probabilities from the base model (3), the filled triangle and circle represent predicted probabilities under a model including the two-way interaction between a single missing ellipse and designs. Plots with trend and shape aesthetics are the least affected by the imbalance in groups, while plots with color aesthetics show huge differences in the predicted probability.